Stratigraphic framework, structural setting, and timing of VMS, epithermal, and porphyry mineralization in the Kitsault River area, northwestern British Columbia

E.A. Miller[1, a], M.D. Ferri[1], B.I. van Straaten[1], and C. Wall[2]

[1] British Columbia Geological Survey, Ministry of Mining and Critical Minerals, Victoria, BC, V8W 9N3
[2] Pacific Centre for Isotopic and Geochemical Research, Department of Earth, Ocean and Atmospheric Sciences, The University of British Columbia, Vancouver, BC, V6T 1Z4
[a] corresponding author: Emily.X.Miller@gov.bc.ca

Recommended citation: Miller, E.A., Ferri, M.D., van Straaten, B.I., and Wall, C., 2025. Stratigraphic framework, structural setting, and timing of VMS, epithermal, and porphyry mineralization in the Kitsault River area, northwest British Columbia. In: Geological Fieldwork 2024, British Columbia Ministry of Mining and Critical Minerals, British Columbia Geological Survey Paper 2025-01, pp. 17-47.

Abstract

The Stikine terrane (Stikinia) of northwest British Columbia hosts significant porphyry, epithermal, and volcanogenic massive sulphide (VMS) precious and base metal deposits. New U-Pb zircon geochronology, mapping, and stratigraphic work in the Kitsault River area provide a framework for understanding the geological setting of the Hazelton Group and distribution of latest Triassic to Early Jurassic mineral deposits in the area. The base of the Hazelton Group consists of local coarse sedimentary rocks of the Kinskuch unit (latest Triassic), which we consider a regional correlative of the Jack Formation. The lower part of the Hazelton Group (Betty Creek Formation; latest Triassic to Early Jurassic, ca. ≤206-190 Ma) records a period of prolific volcanism that almost completely overlaps with ages returned from the Texas Creek plutonic suite (ca. 204.6-191.7 Ma), which hosts and is coeval with porphyry Cu-Au mineralization and epithermal Au mineralization in the map area. A gap of as much as 20 m.y. separates the lower and upper parts of the Hazelton Group throughout much of the map area. However, from Kitsault Lake north to White Lake, a gap of ≥2 m.y. separates a belt of Kitsault unit felsic, intermediate, and mafic volcanic rocks and lower Hazelton Group rocks of the Betty Creek Formation. The Kitsault unit is broadly coeval with the arc-like rocks of the Horn Mountain Formation in the upper part of the Hazelton Group along the Stikine arch and the Iskut River Formation of the Eskay rift. It is coeval with VMS and epithermal Ag-Zn-Pb mineralization in the map area. The uppermost Hazelton Group units are the Smithers Formation (ca. ≤169 Ma) and an unnamed volcano-sedimentary unit (ca. 159 to ≤155 Ma; Middle to Late Jurassic) that occupies the same stratigraphic position as the Quock Formation (Early to Middle Jurassic) as described in central north Stikinia but is younger and coarser-grained. The age of a tuff retrieved from near the base of this unnamed unit is up to 10 million years younger than that of the Kitsault, unit, suggesting that it corresponds to a separate volcanic event and roughly corresponds to Jurassic magmatic pulses in the Coast Plutonic Complex. The host rock for the Ajax porphyry Mo deposit has an Eocene age (ca. 55.5 Ma) and is considered part of the Alice Arm plutonic suite. Structurally controlled mineralization at Surebet is hosted predominantly in the unnamed volcano-sedimentary unit and overlying Bowser Lake Group and is coeval with the Alice Arm and Hyder plutonic suites.

Keywords: Kitsault River, Hazelton Group, Stuhini Group, Betty Creek Formation, Kinskuch unit, Kitsault unit, Smithers Formation, Stikinia, Triassic, Jurassic, U-Pb zircon geochronology, stratigraphy, VMS, porphyry, Golden Triangle, silver, copper, gold

1. Introduction

The Stikine terrane (Stikinia) of northwest British Columbia hosts significant porphyry, epithermal, and volcanogenic massive sulphide (VMS) precious and base metal deposits (Figs. 1, 2), including Schaft Creek, Galore Creek, Red Chris, KSM, Red Mountain, Premier, Snip and Bronson Slope. Particularly significant in the metallogeny of the region are the volcano-sedimentary rocks of the Hazelton Group and coeval plutonic rocks (latest Triassic to Middle Jurassic; Nelson et al., 2013; Logan and Mihalynuk, 2014; Nelson and van Straaten, 2020). The latest Triassic to Early Jurassic was a prolific period of porphyry emplacement associated with Hazelton arc magmatism during which most of the known copper mineralization in British Columbia was emplaced (Logan and Mihalynuk, 2014). Most of the Mesozoic VMS mineralization in Stikinia, including the Eskay Creek and Anyox deposits, is hosted in rift-related rocks of the Iskut River Formation (Middle Jurassic) in the upper part of the Hazelton Group (Fig. 2; Gagnon et al., 2012; Nelson et al., 2013; Nelson et al., 2018). Recent work has recognized significant arc-like volcanic rocks of the upper part of the Hazelton Group such as the Horn Mountain Formation (Fig. 2; van Straaten et al., 2022; van Straaten, 2024; and references therein) and the Kitsault unit, which is associated with VMS and epithermal deposits in the Kitsault River area (Hunter and van Straaten, 2020; Miller et al., 2023). Subsequent deformation, including that of the Skeena fold-and-thrust belt, has obscured the setting and controls on emplacement of these mineral deposits (Evenchick et al., 2007; Miller et al., 2020; Miller et al., 2023). The latest Triassic to Jurassic volcano-sedimentary successions are cut by intrusive rocks of the Hyder plutonic suite (Eocene), which define the western boundary of

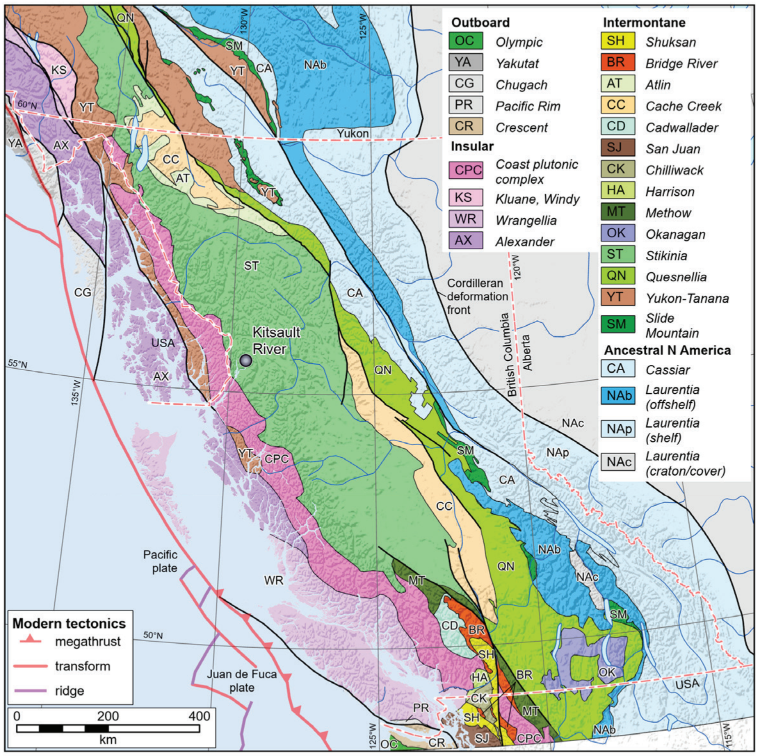

Fig. 1. Location of Kitsault River area. Terranes after Colpron (2020).

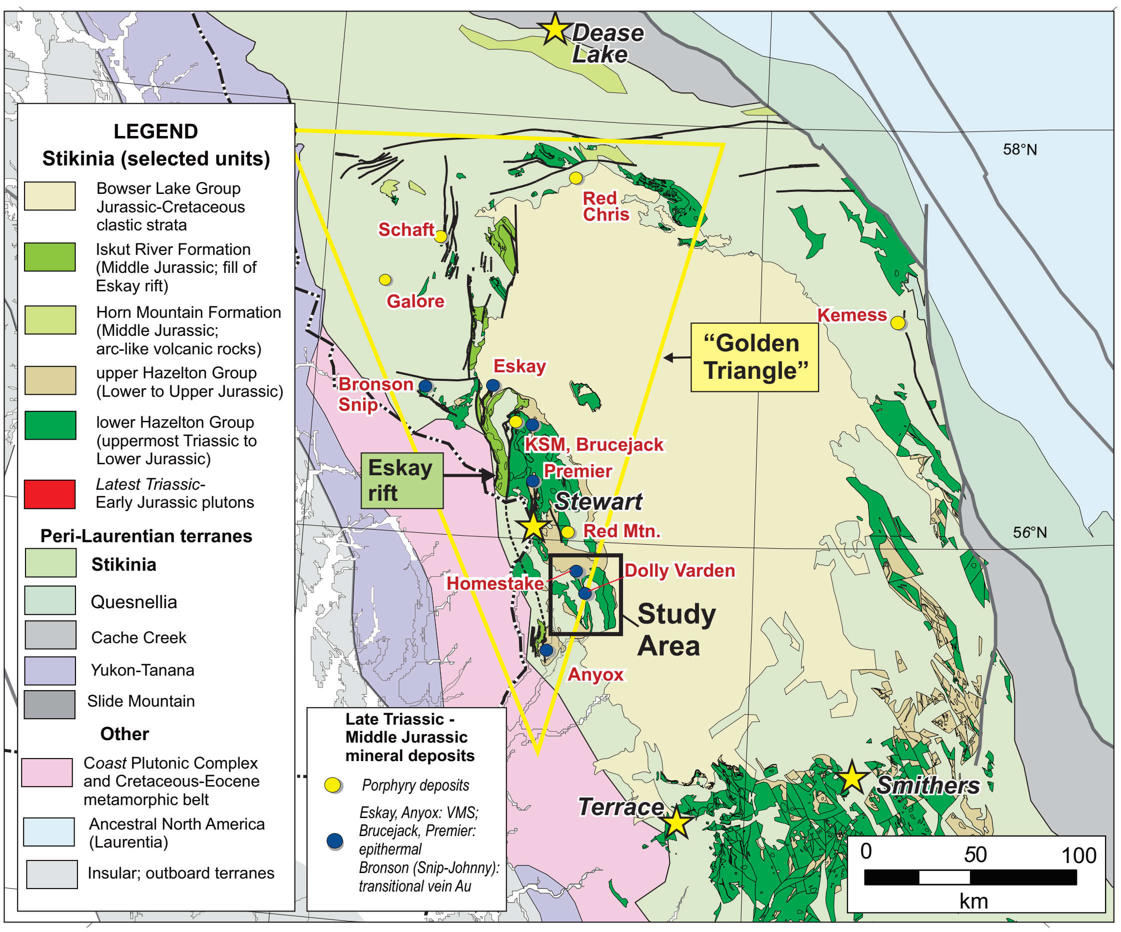

Fig. 2. Regional geological setting with selected mineral deposits. After Nelson et al. (2022).

the map area as part of the Coast Plutonic Complex, and the Alice Arm plutonic suite (Eocene), which host molybdenum porphyries including the past-producing Kitsault deposit.

As part of a multi-year project, detailed bedrock mapping in the Kitsault River area has been directed at resolving the age and affinity of Hazelton Group rocks that host porphyry, epithermal and VMS showings, and testing regional Hazelton Group correlations. Establishing the stratigraphic, magmatic, structural, and chronological framework of rocks in the Kitsault River area will aid understanding of the distribution of mineral deposits in northwestern British Columbia. Based on fieldwork completed in 2019-2024, herein we present a new preliminary geological map (Fig. 3), new geochronology, and an updated stratigraphic framework for the Kitsault River area.

2. Geological setting

The Kitsault River map area is in northwestern British Columbia along the west-central margin of Stikine terrane (Stikinia), in the Intermontane belt of the Canadian Cordillera (Figs. 1, 2), in the traditional lands of the Nisga'a, Gitanyow, Tsetsaut, Skii Km Lax Ha, and Metlakatla First Nations. It is at the southern end of a region popularly referred to as the 'Golden Triangle', a loosely defined area that includes most of the major gold, copper, and silver deposits in west central Stikinia (Fig. 2). Stikine terrane is a multi-episodic island arc tectono-stratigraphic belt that comprises three unconformity-bounded volcano-sedimentary successions: the Stikine assemblage (Paleozoic), Stuhini Group (Late Triassic) and Hazelton Group (latest Triassic -Middle Jurassic). These arc-related rocks are overlain by siliciclastic rocks of the basal Bowser Lake Group (Upper Jurassic). The Kitsault River map area is bounded to the north, east, and south by the Bowser Lake Group, and to the west by Eocene intrusions of the Coast Plutonic complex (Nelson et al., 2013).

The oldest rocks exposed in the map area are sedimentary and arc-related mafic volcanic rocks of the Stuhini Group (Carnian to Norian; Figs. 3, 4). Regionally, cessation of the Stuhini-Takla arc at the end of the Triassic coincides with deformation and a regional unconformity across most of northern Stikinia, attributed to collision between the Yukon-Tanana and Stikine terranes (Nelson et al., 2022). The Stuhini Group is generally unconformably overlain by intermediate volcano-sedimentary rocks in the lower part of the Hazelton Group (Rhaetian to Pliensbachian; e.g., Nelson and Kyba, 2014; Nelson et al., 2018), although locally in the Kitsault River area the Stuhini-Hazelton contact is gradational and conformable (Miller et al., 2023). The transition from Stuhini Group deposition to Hazelton Group volcanism in the latest Triassic and Early Jurassic marks a major tectono-magmatic shift, which corresponds to the most prolific time of porphyry emplacement in British Columbia (ca. 211-199 Ma; Logan and Mihalynuk, 2014; Nelson and van Straaten, 2020; Nelson et al., 2022).

The Hazelton Group has been subdivided into upper and lower parts (Gagnon et al., 2012; Nelson et al., 2018), with most arc volcanic units in the lower part and post-arc sedimentary, rift-related and local arc or arc-like successions in the upper part. Basal rocks in the lower part include coarse-grained siliciclastic rocks, such as the Snippaker unit and Jack Formation in the Bronson-KSM area (Fig. 2; Rhaetian and Sinemurian; Nelson et al., 2018) and the Kinskuch unit in the Kitsault area (Fig. 3; Late Norian to Rhaetian; Miller et al., 2020; Miller, 2023). The basal units are overlain by intermediate volcanic, and lesser felsic and mafic volcanic and volcanic-derived sedimentary rocks (Rhaetian to Pliensbachian; Klastline and Betty Creek formations; Nelson et al., 2018). The regionally developed Tatogga and Texas Creek plutonic suites (latest Triassic to Early Jurassic) are coeval and comagmatic with volcanic units in the lower part of the Hazelton Group (Nelson et al., 2018). This magmatism is associated with significant latest Triassic to Early Jurassic porphyry copper-gold and related epithermal gold deposits (Fig. 2) including Red Chris, Red Mountain, Premier, KSM (Kerr-Sulphurets-Mitchell-Snowfield-Iron Cap) and Brucejack. In the Kitsault River map area, latest Triassic to Early Jurassic mineralization includes the Big Bulk porphyry Au-Cu system (Fig. 3; MINFILE 103P 014), and the Homestake Ridge epithermal Au-Ag-Cu deposit (Fig. 3; MINFILE 103P 216; for more details see Perry and Febbo, 2017; Hunter and van Straaten, 2020; Miller, 2023 and references therein). Syndepositional faults influenced the deposition and distribution of the basal Hazelton Group (Jack Formation and Kinskuch unit) and controlled emplacement of latest Triassic to Early Jurassic intrusions that caused porphyry and epithermal mineralization (Nelson and Kyba, 2014; Febbo et al., 2019; Miller et al., 2020; Nelson and van Straaten, 2020; Miller, 2023).

Regionally, the upper part of the Hazelton Group (Pliensbachian to Bajocian) unconformably overlies the lower Hazelton Group. It comprises post-arc sedimentary rocks of the Spatsizi, Smithers, and Quock formations (Pliensbachian to Callovian; Gagnon et al., 2012), local bimodal rift-related volcanic and sedimentary rocks of the Iskut River Formation (ca. 179-173 Ma; Nelson et al., 2018, and references therein), and the broadly coeval, arc-like volcanic rocks of the Horn Mountain Formation (ca. 185-171 Ma; van Straaten et al., 2022; van Straaten, 2024), Mount Dilworth Formation (ca. 173.6 Ma; Cutts et al., 2015; Alldrick, 1993), and the Kitsault unit (ca. ≤188 to ≤168 Ma; Hunter and van Straaten, 2020; Miller et al., 2023). The Iskut River Formation hosts several mineral deposits such as VMS-style mineralization at the Au-Ag-rich Eskay Creek and Cu-rich Anyox deposits in the Eskay rift (Fig. 2; Barrett and Sherlock, 1996; Childe, 1996; Macdonald et al., 1996; Roth et al., 1997; Evenchick and McNicoll, 2002). Bowser Lake Group (Middle Jurassic to mid-Cretaceous) siliciclastic sedimentary rocks overlie the Hazelton Group and record the accretion of Stikinia to Ancestral North America and deposition of erosional products from the orogen into a foreland basin (Evenchick and Thorkelson, 2005; Evenchick et al., 2007)

Intense shortening and crustal thickening in the mid-Cretaceous during the assembly of the Canadian Cordillera into an accretionary orogen was expressed in this region by the

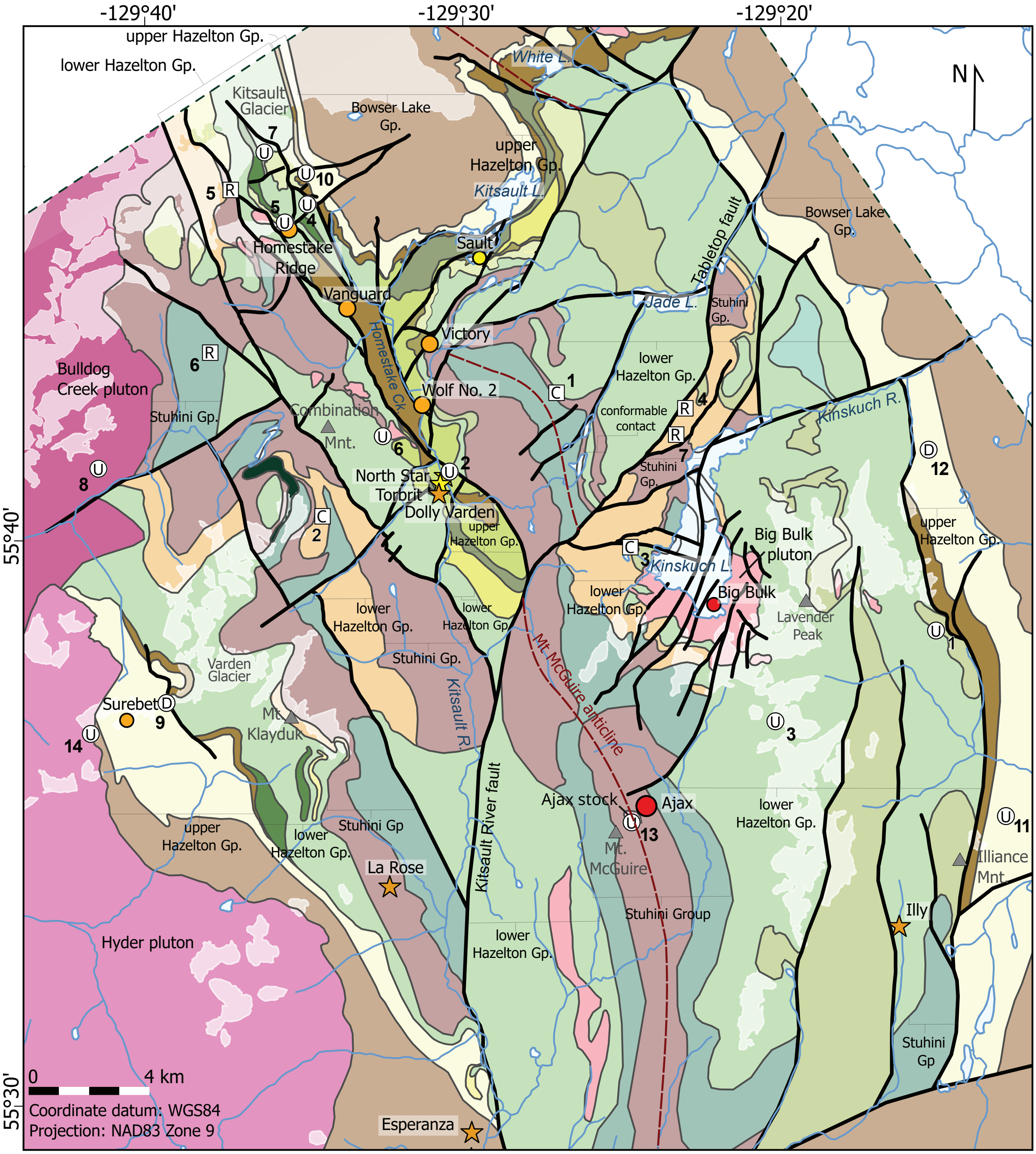

Fig. 3. Geologic map of the Kitsault River area. Locations of fossil age samples listed in Table 1; new geochronologic dates listed in Table 2.

Fig. 3. Continued. Legend for Figures 3 and 4.

development of the thin-skinned Skeena fold-and-thrust belt. Deformation in the belt is expressed as a wide variety of fault and fold geometries and styles, as a function of competency contrast (Evenchick, 1991; Evenchick et al., 2007). Initiating in the Late Cretaceous and continuing into the Eocene, significant dextral offset accumulated along large-scale faults that appear to have reactivated pre-existing orogen-parallel structures (Nelson and Kyba, 2014).

Eocene porphyry systems in the area are hosted in the stocks of the Alice Arm plutonic suite. These low F-type porphyry molybdenum systems (Orovan et al., 2024) include the past-producing Kitsault (MINFILE 103P 120) and Tidewater (MINFILE 103P 111) mines, and Ajax deposit (MINFILE 103P 223). These deposits are commonly cut by Ag-Pb-Zn±Au-bearing veins, which may represent late-stage porphyry veins and/or a later mineralization event (LeBel, 1988; Giroux and L'Heureux, 2007; Orovan et al., 2024). The western margin of the map area is bounded by the Hyder pluton (Eocene) of the Coast Plutonic complex.

3. Geology of the Kitsault River area

3.1. Stuhini Group (Upper Triassic)

The oldest rocks in the map area are of the Stuhini Group (Upper Triassic), exposed in the core of the regional Mount McGuire anticline (Dawson and Alldrick, 1986), which trends sub-parallel to Kitsault River (Fig. 3). These rocks include a lowermost, aerially extensive sedimentary unit, overlain by a mafic volcanic unit and local mafic subvolcanic intrusions. The sedimentary unit includes laminated to thinly bedded argillite, mudstone, and siltstone with lesser sandstone, pebbly sandstone, sandy limestone, and rare chert. Argillite and mudstone are locally graphitic. Coarse-grained sedimentary rocks are more commonly observed near the top of the Stuhini Group. Conodonts collected from carbonate-rich strata in the Stuhini Group consistently return Carnian to Rhaetian ages (Table 1; Fig. 4; Golding et al., 2019; this study). The volcanic unit comprises augite-feldspar-phyric mafic coherent flows, massive lapilli tuff and volcanic breccia locally interstratified with the sedimentary unit (Fig. 5). A chert bed sampled from a mafic tuff to tuff breccia succession in the Surebet/Homestake

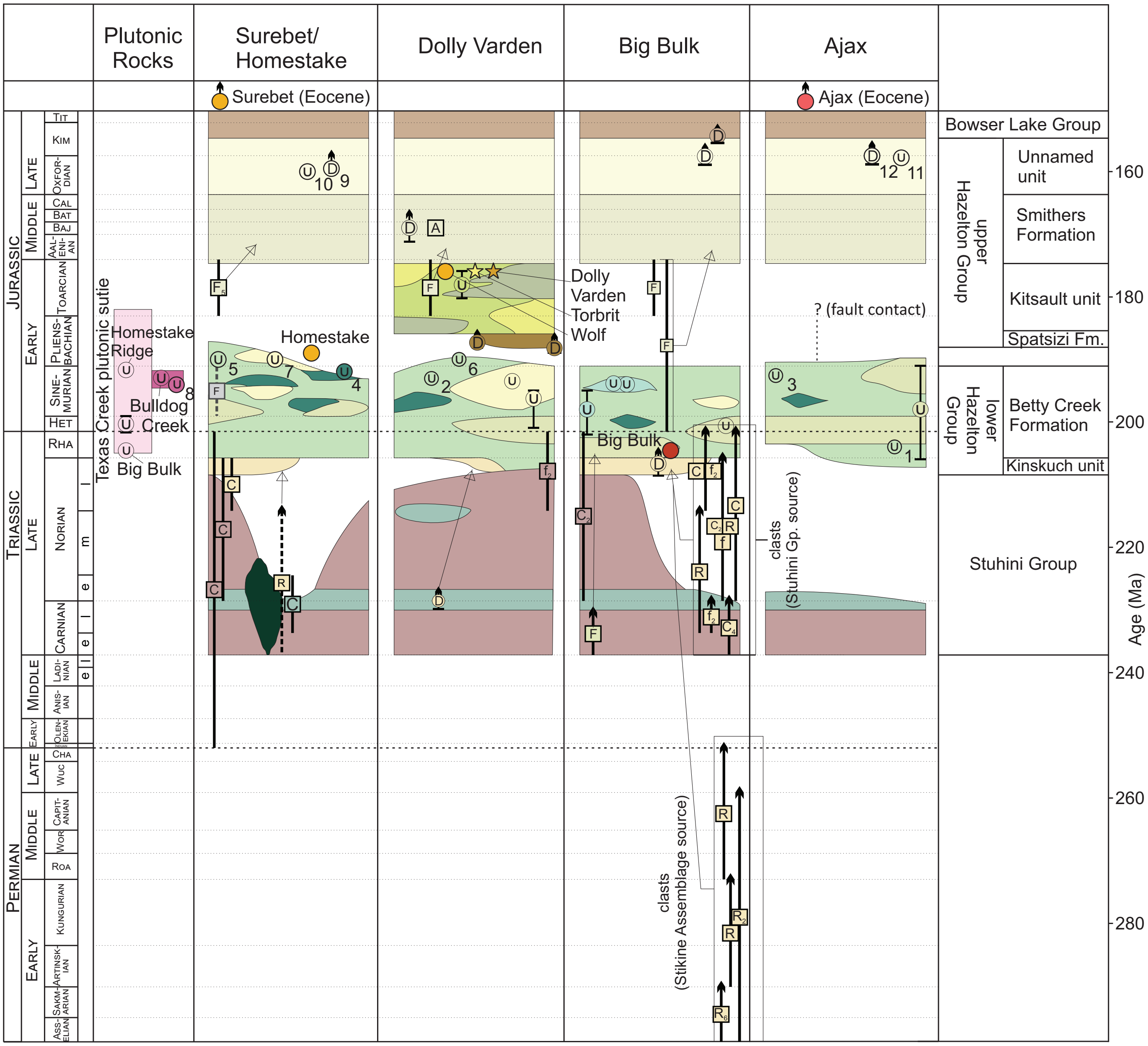

Fig. 4. Permian to Jurassic stratigraphic and magmatic framework for the Kitsault River area. Geochronological samples (circles): U = U-Pb zircon, D = detrital zircon (arrow on all denotes maximum depositional age, MDA), Fossil samples (squares): F = macrofossil, A = ammonoid, C = conodont, subscript = number of collections, dashed black lines = probable age, upward arrow on fossil age line denotes sample from a conglomerate clast (see arrow tie-lines to unit source) = MDA (Late Triassic ages interpreted as clasts sourced from Stuhini Group, Permian ages interpreted as chert clasts sourced from Stikine assemblage basement). Bold outlines indicate new geochronological data presented in this study. Selected deposits placed in their inferred approximate stratigraphic position and age: star = past producer, circle = project, red = porphyry, orange = vein hosted, yellow = massive sulphide. Geological time scale after Cohen et al. (2013). Legend shared with Figure 3. Historical fossil data compiled from Cordey et al. (1992); Greig (1992); Golding et al. 2023. Geochronological data compiled from Greig and Gehrels (1995), Hunter et al. (2020, 2022a, 2022b), Miller et al. (2020, 2023). Ages with subscripts are from this study (see Tables 1, 2). Approximate location of the areas for each generalized section are labeled in Figure 3.

area returned late Carnian to early Norian radiolaria and constrains Stuhini Group volcanism in the area (Table 1; Golding et al., 2023). The study area is considered to have been in a relatively quiescent back-arc basin setting in the Late Triassic with limited volcanic input, due in large part to the relatively high proportion of fine-grained sedimentary strata relative to volcanic strata along the Stikine arch (Nelson and van Straaten, 2020).

Low volume augite-phyric dikes and sills cut Stuhini Group sedimentary and volcanic strata in the northwest part of the map

Table 1. Summary of microfossil ages by geological unit. Sources: 1- Golding (2023); 2- Golding (2024); 3- Golding et al. (2023); 4- Cordey (2020); 5- Cordey (2023).

Sample	No.	Period/ Epoch	Age	Type	Lithostratigraphic unit	Longitude*	Latitude*
22RHU-058f	1	Upper Triassic	Late Norian to Rhaetian[1]	Conodont	Kinskuch unit (uTrHKscb)	-129.449614	55.711689
23MFE-20a	2	Upper Triassic	Late Norian[2]	Conodont	Kinskuch unit (uTrHKscb)	-129.571368	55.674758
17-HMC-18-114	3	Upper Triassic	Norian[3]	Conodont	Kinskuch unit (uTrHKscb)	-129.410594	55.666299
19EMI-8-48	4	Upper Triassic	Late Carnian to mid-Norian[4]	Radiolarian	Kinskuch unit (uTrHKscb)	-129.382268	55.707337
23EMI-30a	5	Upper Triassic	Early Carnian to mid-Norian[5]	Radiolarian	Stuhini Group (uTrSsf)	-129.620818	55.770739
23BVA-13a	6	Upper Triassic	Late Carnian to early Norian[5]	Radiolarian	Stuhini Group (uTrSvb)	-129.630765	55.722718
18EMI-4-28	7	Permian	Artinskian to Kungurian[4]	Radiolarian	Kinskuch unit (uTrHKscb)	-129.386997	55.699568

*Datum used for all coordinates: WGS 1984

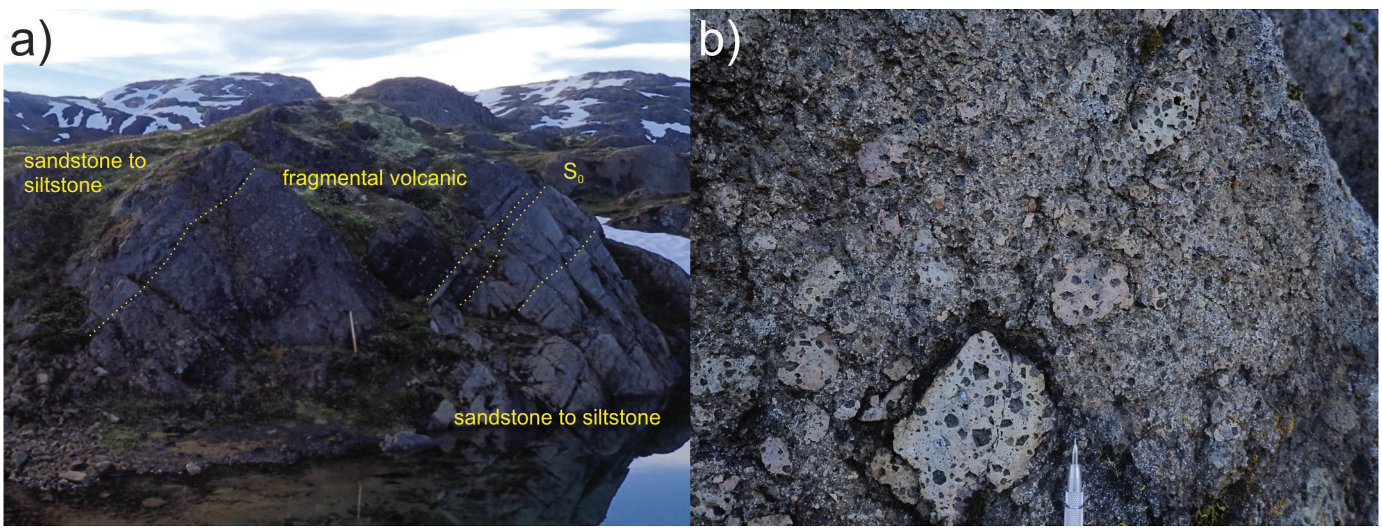

Fig. 5. Stuhini Group. **a)** Interstratified laminated to thinly bedded sandstone and siltstone of the Stuhini Group sedimentary unit and beds of the mafic volcanic fragmental unit. Photo taken facing E at 55.69321°N, 129.441263°W. **b)** Groundmass-supported lapilli tuff of mafic volcanic fragmental unit; both groundmass and lapilli are augite phyric. Lapilli display cuspate-lobate margins consistent with interpretation as juvenile volcanic clasts; some have calcite-filled amygdules. Photo taken facing SE at 55.693377°N, 129.441377°W.

area in the Surebet/Homestake area (Figs. 3, 4). These dikes are texturally and compositionally indistinguishable from coherent Stuhini volcanic rocks except where sharp intrusive contacts with surrounding Stuhini Group rocks are observed. They are interpreted as feeders to Stuhini Group volcanism.

3.2. Hazelton Group

3.2.1. Lower part of Hazelton Group

The Stuhini Group is overlain by volcanic and sedimentary rocks in the lower part of the Hazelton Group (latest Triassic to Early Jurassic). Approximately 4 km southwest of Jade Lake, Hazelton Group volcanic rocks interfinger with the Stuhini Group sedimentary rocks indicating a conformable contact (Figs. 3, 4). However, near Kinskuch Lake, the Kinskuch unit records a marked sub-Hazelton Group unconformity, and 8 km southwest of Homestake ridge, laminated to bedded siltstones and sandstones of the Stuhini Group are abruptly overlain by Betty Creek Formation volcanic conglomerate to andesitic tuff breccia that cut into the underlying sedimentary rocks, consistent with a sub-Hazelton Group unconformity (Fig. 6), and locally in the Big Bulk and Ajax-Illy areas, basal Hazelton Group rocks abruptly overlie the Stuhini volcanic unit along a sharp contact that we interpret as an unconformity (Figs. 3, 4)

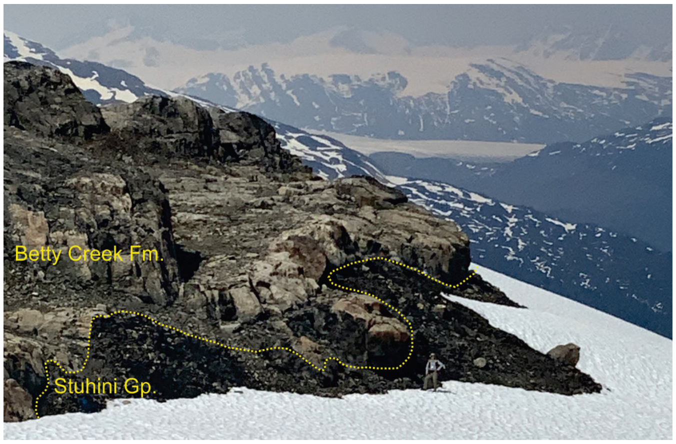

Fig. 6. Contact between Betty Creek Formation andesitic fragmental volcanic rocks, and Stuhini Group siltstone to fine sandstone. The base of the volcanic sequence cuts into the underlying sedimentary rocks (yellow line). Facing N at 55.681286°N, 129.593108°W.

3.2.1.1. Kinskuch unit (uppermost Triassic)

The base of the Hazelton Group in the map area locally comprises a discontinuous package of coarse sedimentary rocks informally referred to as the Kinskuch unit (Miller et al., 2020; latest Triassic). The unit includes massive to poorly stratified conglomerate, megaclast-bearing conglomerate (with clasts up to 120 m; Fig. 7a), well-stratified pebbly sandstone, sandstone, and rare mudstone. The unit ranges from only a few m thick to at least 300 m thick near Kinskuch Lake (Fig. 4). It occupies a roughly v-shaped geometry apparently related to intersecting NE-NW fault systems, is absent in the core of the map area, and its distribution has been shown to be controlled by synsedimentary faults near Kinskuch Lake (Fig. 3; Miller, 2023). The unit is poorly to very poorly sorted; clasts range from rounded to angular and include sandstone, mudstone, limestone, chert, augite-phyric mafic volcanic, and hornblende-feldspar-phyric intermediate volcanic rocks (Figs. 7b, c). Clast composition and size vary rapidly both along strike and up stratigraphy. Quartz grains are rare. Clasts are interpreted to be sourced from uplift and erosion of Stuhini Group and older rocks as well as volcanic input from coeval lower Hazelton Group volcanism, because hornblende-bearing rocks were only observed in Hazelton Group rocks and co-magmatic intrusions (Miller et al., 2020; Miller, 2023). The Kinskuch unit is considered latest Triassic based on late Norian to Rhaetian conodonts from a limestone megaclast at the base of the unit (GSC no. C-178198; Golding et al., 2023; Table 1) and by a U-Pb zircon age of ca. 204.6 Ma from the Big Bulk stock, which cuts the upper contact of the unit with overlying Betty Creek Formation andesite (Miller et al., 2020). Some chert clasts returned Permian radiolaria (Table 1; Golding et al., 2023), presumably implying derivation from the Stikine assemblage.

3.2.2.2. Betty Creek Formation (uppermost Triassic to Lower Jurassic)

The Kinskuch unit is conformably overlain by the Betty Creek Formation (uppermost Triassic to Lower Jurassic; (Figs. 3, 4), a varied volcano-sedimentary package that includes andesitic, tuffaceous sedimentary, mafic volcanic, K-feldspar phyric volcanic, and felsic volcanic subunits.

The andesitic subunit (ca. 206.7-193.5 Ma, Hunter and van Straaten, 2020; Hunter et al., 2022a; this study) volumetrically comprises most of the Betty Creek Formation. It includes massive to very thickly bedded (5-100 m) intermediate fragmental volcanic rocks including green to maroon massive andesitic lapilli-tuff, lapillistone, tuff breccia, and lesser crystal tuff (Fig. 8). The subunit also includes rare ~0.2 to 1 m thick and ~0.5-5 m wide sandstone channels, 0.5 to 10 m thick beds of sandstone and reworked epiclastic strata, and thin (<2 m) tuff beds. Clasts are angular to subrounded, hornblende-plagioclase-phyric with lesser amygdaloidal mafic and maroon juvenile clasts and rare sandstone, argillite, limestone and augite-phyric volcanic accessory clasts in a crystal and/or ash matrix.

The tuffaceous sedimentary subunit (ca. 204-200 Ma; Greig et al., 1995; Greig and Gehrels, 1995; Hunter et al., 2022a, b; this study) is discontinuous throughout much of the map area but is locally mappable at 1:50,000 scale at the base of the Betty Creek Formation in the Big Bulk and Dolly Varden areas and at higher stratigraphic levels in the Big Bulk and Ajax/Illy areas (Figs. 3, 4). It comprises well-stratified to locally massive green to maroon sedimentary and maroon, green and pale weathering volcanic rocks including coarse- to fine-grained feldspathic sandstone, siltstone, conglomerate, and limestone, intercalated with andesitic tuff and tuff breccia and lesser felsic and mafic tuff similar in character to the volcanic rocks of the andesitic, felsic and mafic volcanic subunits (Fig. 9). The volcanic components are similar to interfingering andesitic, felsic, and mafic volcanic subunits.

The K-feldspar-phyric volcanic subunit (ca. 194 Ma; Hunter et al., 2022, a, b) is confined to a single outcrop area 3 km northeast of Kinskuch Lake (Fig. 3). It consists of distinctly K-feldspar-hornblende-plagioclase phyric to K-feldspar megaphyric coherent andesite, and K-feldspar crystal tuff (Fig. 10) intercalated with 100 m-thick lapilli-tuff to tuff breccia intervals with hornblende plagioclase-phryic volcanic clasts (similar to the andesitic volcanic subunit), and rare local lenticular and discontinuous beds of brown weathering coarse- to very coarse-grained sandstone. The long axis of K-feldspar phenocrysts commonly lie along bedding. This unit is interpreted to record the eruption of a single, short-lived volcanic centre.

The mafic subunit comprises dark green to black to lesser dark-maroon mafic coherent flows and flow-top breccias, tuff,

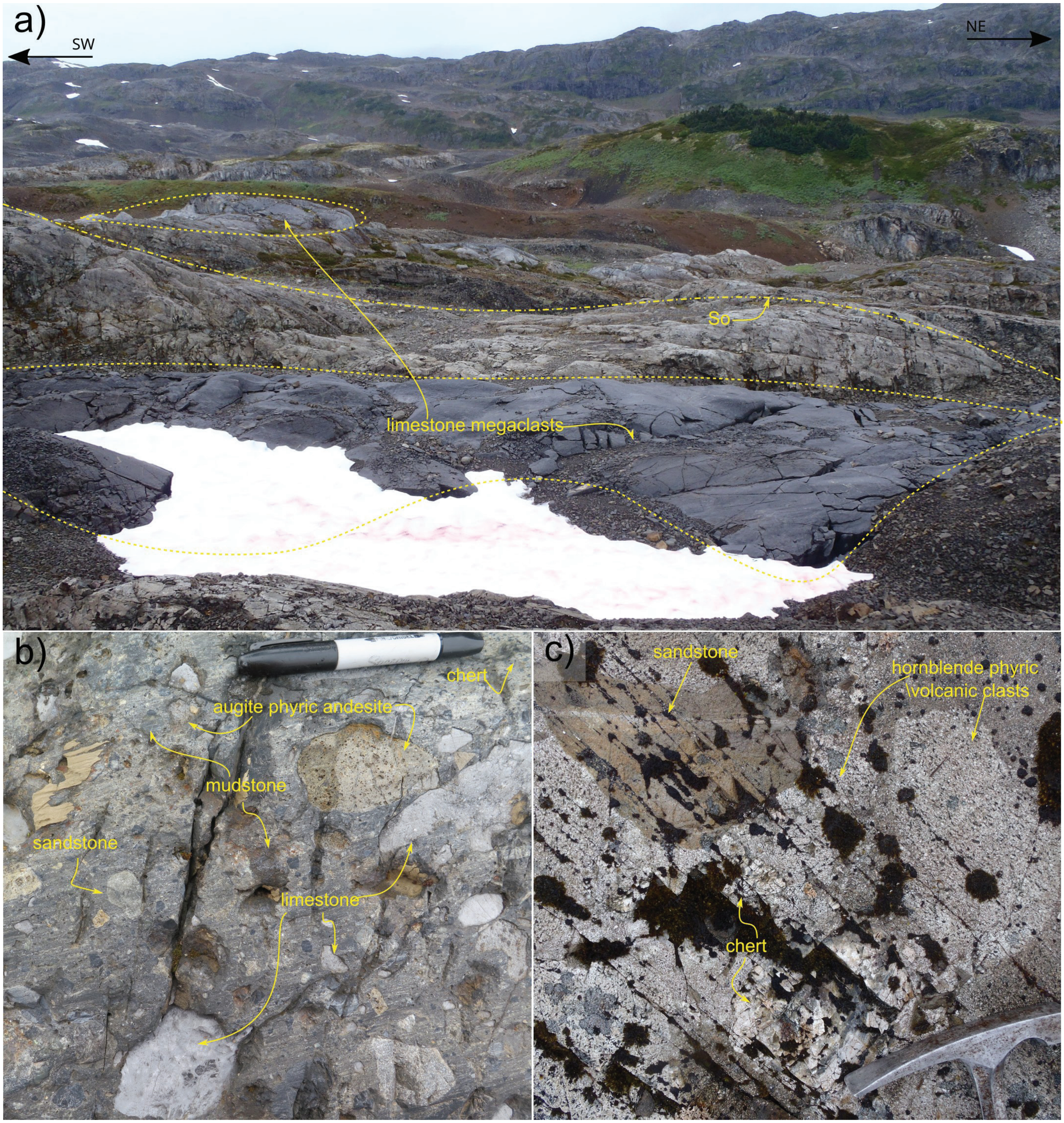

Fig. 7. Kinskuch unit. **a)** Megaclast of dark grey massive to very thickly bedded limestone in conglomerate near Kinskuch Lake, near the base of the Kinskuch unit. The surrounding conglomerate is polymictic pebble to cobble conglomerate, including Stuhini Group sourced and intraformational clasts in a framework-supported sandstone matrix. Taken facing NW at 55.681639°N, 129.393452°W. **b)** Polymictic pebble to cobble conglomerate with clasts of clastic sedimentary rocks, limestone, chert, and augite-phyric volcanic rocks interpreted as being sourced from uplift and erosion of underlying Stuhini Group rocks. Photo taken facing W at 55.647393°N, 129.397113°W. **c)** Matrix-supported polymictic cobble to pebble conglomerate with sandstone and chert clasts (interpreted as being sourced from Stuhini Group) and hornblende-phyric volcanic clasts (interpreted as intraformational Hazelton Group clasts) in a framework-supported pebbly sandstone matrix. Photo taken looking down with N at the top of the photo at 55.682534°N, 129.394829°W.

Fig. 8. Betty Creek andesite subunit. A friable maroon lapilli tuff containing rare white mica; geochronology sample 1 (22BvS-90b). Facing E at 55.642169°N, 129.250686°W.

Fig. 9. Betty Creek Formation volcano-sedimentary subunit. Well stratified volcanic-derived sedimentary rocks. Beds dip to the east. The rock comprises maroon cobble conglomerate, fine sandstone, and grey-brown limestone interstratified with pale to white weathering beds that are likely tuff or reworked tuff. Facing S at 55.546060°N, 129.319302°W.

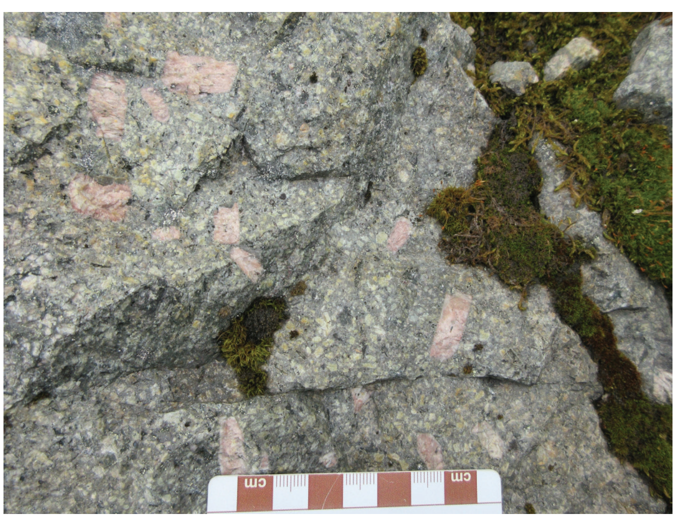

Fig. 10. Betty Creek Formation K-feldspar megacrystic andesite subunit, showing cm-scale K-feldspar megacrysts in a plagioclase-phyric groundmass. Taken at 55.721645°N, 129.335414°W.

lapilli tuff, and volcanic breccia. It is commonly augite-rich (Fig. 11a) and contains mafic juvenile clasts that are commonly amygdaloidal (Fig. 11b).

The felsic subunit (ca. 201-190 Ma; Hunter et al., 2022a, b; this study) comprises light green to grey to maroon-grey felsic lapilli-tuff, crystal tuff, and tuff (Fig. 12) with lesser flow-banded coherent rocks. The subunit locally contains quartz, biotite, K-feldspar, and/or white mica crystals and rare elongate volcanic clasts (to 2 mm), which may represent fiamme. The mafic and felsic volcanic subunits are intercalated with the andesitic subunit and lack significant continuity through much of the map area. Locally they occur as more voluminous and continuous units particularly at or near the top of the Betty Creek Formation in the Dolly Varden and Homestake/Surebet areas (Figs. 3, 4).

3.2.3. Texas Creek plutonic suite (latest Triassic to Early Jurassic)

We distinguish four units in the Texas Creek plutonic suite: the Big Bulk pluton (latest Triassic), several unnamed diorite intrusions (latest Triassic to Early Jurassic), several unnamed monzodiorite bodies (latest Triassic to Early Jurassic), and the Bulldog pluton (Early Jurassic).

The Big Bulk pluton (ca. 204.6 Ma; Miller et al., 2020) is a multiphase diorite stock exposed on the southern shore of Kinskuch Lake (Fig. 3). Based on crosscutting relationships, Perry and Febbo (2017) and Miller (2023) recognized five intrusive phases, all of which display roughly east-west-trending contacts. The phases are similar in composition consisting of crowded, fine- to medium-grained, hornblende-plagioclase phyric diorite and lesser monzonite/monzodiorite, and intrusive breccia with 10-45% plagioclase and 5-25% hornblende phenocrysts (1-6 mm) in a commonly altered fine-grained groundmass of plagioclase, hornblende, and rare (<1%) quartz. The first four phases host the Big Bulk Cu-Au porphyry system. The second phase is inter-mineral and returned the Rhaetian age; it cuts the Stuhini Group, the Kinskuch unit and basal Betty Creek Formation volcanic rocks (Miller, 2023). The fifth phase is post-mineral and characteristically only weakly altered to unaltered.

The unnamed intrusions comprise subvolcanic to plutonic rocks ranging from hornblende diorite, biotite-hornblende monzodiorite, monzonite to lesser quartz monzonite. They occur throughout the entire map area predominantly as small (<5 m wide) bodies. Dikes and stocks that are large or abundant enough to be mappable at 1:50,000 scale are exposed along a roughly northerly trend along the Homestake and Kitsault River valleys, particularly near Homestake ridge, Combination Mountain, and southwest of Mount McGuire (Fig. 3). They are generally quartz poor (<5% quartz) except in rare quartz monzonitic dikes such as those observed in the Homestake ridge area (Fig. 3) and display a wide range of textures and grain sizes. Most are oriented roughly N-S or E-W, similar to the general structural grain (Fig. 3). Stocks and dikes of the Texas Creek plutonic suite cut the rocks of the Stuhini Group and lower part of the Hazelton Group.

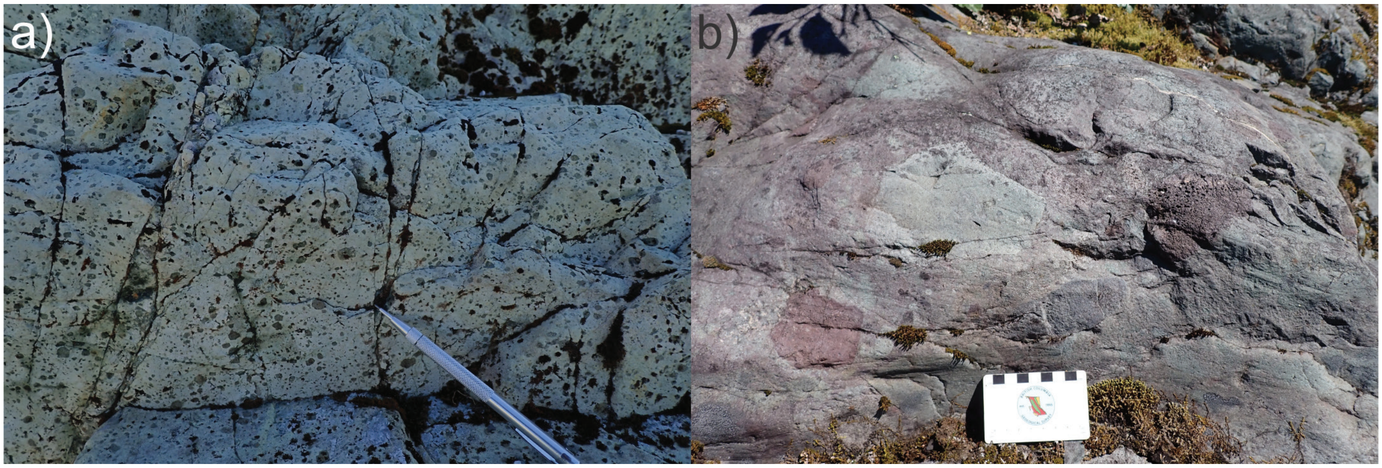

Fig. 11. Betty Creek Formation mafic volcanic subunit. **a)** Coherent volcanic rock with mm- to cm-scale euhedral augite phenocrysts in a fine-grained groundmass. Facing E at 55.59497°N, 129.579025°W. **b)** Tuff breccia with maroon, green, and grey, amygdaloidal clasts in a green to maroon matrix. Taken facing NE at 55.764815°N, 129.573592°W.

Fig. 12. Betty Creek Formation felsic volcanic subunit. Interstratified felsic tuff and volcanic-derived feldspathic sandstone (scoured basal contact below pencil). Bedding orientation is 138°/35°, taken facing S at 55.598286°N, 129.573080°W.

Fig. 13. Bulldog Creek pluton, Texas Creek plutonic suite. Quartz monzonite that is variably hornblende-plagioclase-K-feldspar-quartz-phyric. Geochronology sample 8 collected at 55.688184°N, 129.688536°W.

At the northwest margin of the map area is a large granitoid body named the Bulldog Creek pluton by Greig et al. (1995) with an age of ca. 193-193.8 Ma (Evenchick et al., 2008b; this study). The pluton is white, buff to green weathering and varies from biotite-bearing hornblende quartz monzonite to rare monzogranite. The rocks contain 15-20% and locally up to 30% quartz, with <5% biotite and 10-25% hornblende (Fig. 13) and are medium- to coarse-grained equigranular to porphyritic (locally K-feldspar megacrystic). Moderate to strong epidote-sericite-chlorite alteration is common and the margins of the pluton are typically fault zones. The pluton contains more quartz than most of the other Texas Creek plutonic suite intrusions in the map area. It cuts Betty Creek Formation and Stuhini Group rocks (Fig. 4).

3.2.4. Upper part of the Hazelton Group (Lower to Upper Jurassic)

The Betty Creek Formation is overlain by the upper part of the Hazelton Group (Figs. 3, 4). It consists of the Spatsizi Formation and Kitsault unit, which are only observed in a 15 km-long belt in the north-centre of the map area, and the Smithers Formation and an unnamed volcano-sedimentary unit throughout the entire map area.

3.2.4.1. Spatsizi Formation (Lower Jurassic)

The Spatsizi Formation is only exposed in the Dolly Varden area, along a 9 km belt from south of Kitsault Lake north to White Lake (Fig. 3) where it is 20-100 m thick and includes well-stratified black mudstone, siliceous siltstone, limestone, feldspathic wacke, and conglomerate, interstratified with minor fine tuff to lapilli-tuff. Mudstone and siltstone are predominant south of Kitsault Lake; coarse-grained sedimentary rocks, including conglomerate, are predominant near White Lake (Fig. 14). The contact between the Spatsizi Formation and underlying Betty Creek Formation is not exposed. However, U-Pb detrital zircon samples from sandstone near the base of the Spatsizi Formation at the Sault showing yielded maximum depositional ages of ca. ≤188 Ma (U-Pb detrital zircon, Hunter et al., 2022a), which is at least several million years younger than the Betty Creek felsic volcanic rocks it overlies. This may suggest an unconformable contact between the upper and lower parts of the Hazelton Group, consistent with observations in other parts of northwestern British Columbia (e.g., Gagnon et al., 2012; Nelson et al., 2018).

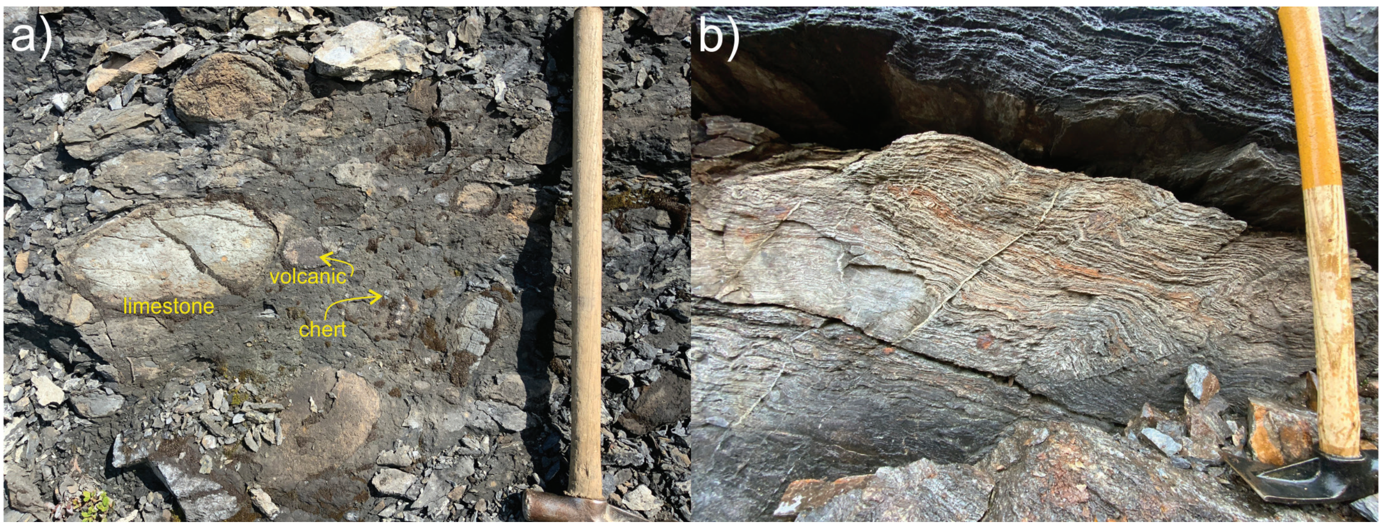

Fig. 14. Spatsizi Formation. **a)** Matrix-supported boulder to pebble conglomerate with limestone, plagioclase-phyric volcanic, chert and rare sulphide clasts in a dark wacke matrix. Taken at 55.792858°N, 129.459931°W. **b)** Laminated graphitic calcareous mudstone and grey limestone that has been deformed. Taken facing NW at 55.751556°N, 129.490264°W.

3.2.4.2.Kitsault unit (Lower to Middle Jurassic)

The Kitsault unit (Lower to Middle Jurassic), named by Hunter et al. (2022b), is a compositionally variable volcanic unit exposed in a 15 km-long belt that extends from White Lake in the north to the confluence of the Kitsault and Homestake rivers along the western limb and axial surface trace of the Mount McGuire anticline. It occupies a triangular, mainly fault-bounded area, the apex of which is 4 km south of Dolly Varden, that widens to the north with the branching termination of the Kitsault River fault (Fig. 3). Texturally and mineralogically, rocks of the Kitsault unit are similar to the volcanic rocks of the Betty Creek Formation and distinguished from them primarily on the basis of stratigraphic position and age. The Dolly Varden deposits (including Dolly Varden, Torbrit, North Star, and Wolf) are coeval with the Kitsault unit and are hosted by the Kitsault unit and underlying Betty Creek Formation in the same fault-bounded area that contains the Kitsault unit. We distinguish three subunits: andesitic volcanic, felsic volcanic, and mafic volcanic.

The andesitic volcanic subunit (ca. 178.1 Ma) is predominant in the central part of the map area in the Kitsault River valley (Fig. 3). It comprises green to grey to grey-maroon intermediate volcanic rocks including tuff, lapilli-tuff, crystal tuff, and local tuff breccia (Fig. 15) interstratified with volcanic-derived sandstone, reworked tuff, and pebble conglomerate with volcanic and sedimentary clasts and rare discontinuous felsic volcanic rocks similar to the felsic volcanic subunit.

The felsic volcanic subunit is most prominent along a 5 km-long corridor from the southeast of Kitsault Lake at the Sault showing north to White Lake (Fig. 3). At the Wolf deposit and farther south the subunit is discontinuous (McCuaig and Sebert, 2017; this study). The subunit comprises predominantly felsic volcanic rocks interstratified with lesser intermediate

Fig. 15. Andesitic subunit, Kitsault unit. Tuff breccia containing a variety of intermediate and lesser mafic volcanic clasts including lapilli, blocks, and bombs. Intermediate clasts contain variable amounts of medium- to coarse-grained hornblende and plagioclase; mafic clasts are commonly amygdaloidal and contain rare augite. Taken facing S at 55.666757°N, 129.476193°W.

and rare mafic volcanic rocks including pale greenish, grey to cream tuff breccia, lapilli-tuff, lapillistone, and crystal tuff (Fig. 16) interstratified with rare sandstone and limestone. Plagioclase-phyric volcanic clasts set in a plagioclase crystal-bearing matrix are common. The subunit is locally foliated or contains elongated volcanic clasts, which may be represent fiamme and/or a tectonic fabric.

Fig. 16. Felsic subunit, Kitsault unit. Felsic lapilli tuff showing alignment of elongated lapilli. Taken facing S at 55.79575°N, 129.453597°W.

The mafic volcanic subunit is exposed along a 7 km-long corridor stretching from southwest of Kitsault Lake to White Lake in the north (Fig. 3). In the hanging wall of the Dolly Varden, Torbrit, and North Star deposits, the subunit is more discontinuous (McCuaig and Sebert, 2017; Hunter et al., 2022b). The subunit contains dark green to black mafic volcanic rocks including lapilli-tuff and tuff breccia, with variable amounts of augite-phyric to aphyric volcanic clasts, and augite-phyric coherent volcanic rocks (Fig. 17), interstratified with lesser limestone, siltstone, feldspathic wacke, and rare conglomerate (Hunter et al., 2022b).

The lower contact of the Spatsizi Formation with the Betty Creek Formation is unexposed but is considered an unconformity because of the geochronological gap described above. The upper contact of the Spatsizi Formation and the overlying Kitsault unit is also unexposed but was interpreted as conformable based on descriptions of interstratification in drill core (McCuaig and Sebert, 2017).

3.2.4.3. Smithers Formation (Middle Jurassic)

The Smithers Formation is observed near the top of the upper Hazelton Group throughout the entire map area and consists of fine- to coarse-grained, well-stratified mudstone to feldspathic wacke, pebbly wacke, carbonate-rich fossiliferous conglomerate, and limestone. Fossils are common and include belemnites (Fig. 18a), bivalve fragments, corals and rare ammonoids. The belemnites are characteristic and serve as a useful marker for the unit. It ranges from a few m to an apparent thickness of 1 km north of White Lake. Some of this variation may be due to structural thickening. Tight to isoclinal folds are

Fig. 17. Mafic subunit, Kitsault unit. Mafic tuff breccia with augite-plagioclase-phyric clasts; 0.5-2 mm equant hexagonal augite phenocrysts in clasts. Taken facing NW at 55.800544°N, 129.469208°W.

common, particularly in the fine-grained and carbonate-rich rocks in the Surebet and Homestake areas.

Hunter and van Straaten (2020) reported a ca. ≤168.9 Ma U-Pb detrital zircon maximum depositional age (youngest statistical population) for the Smithers Formation (Middle Jurassic) and the unit appears to conformably overlie the Kitsault unit based on interstratification of tuff and belemnite-bearing sedimentary rocks at Kitsault Lake, and in the Kitsault River valley (McCuaig and Sebert, 2017; Hunter et al., 2022b). On the eastern limb of the Mount McGuire anticline, the Smithers Formation is in fault contact with Betty Creek Formation rocks (Fig. 3). The base of the Smithers Formation in the Homestake area is a belemnite-bearing conglomerate containing angular volcanic clasts likely sourced from the underlying Betty Creek Formation felsic subunit. An exposure at the base of this conglomerate shows an erosional scour into the volcanic rocks (Fig. 18b). There is an approximately 30 m.y. age difference between the underlying Betty Creek Formation volcanic rocks and tuff beds dated from the base of the overlying unnamed volcanosedimentary unit (see below). On this basis the contact between the Smithers Formation and underlying Betty Creek Formation is interpreted as unconformable. This interpretation is consistent with the diachronous ages of uppermost Betty Creek volcanic rocks in stratigraphic contact with overlying Smithers Formation, which range from at least ca. ≤190 Ma to ca. 192 Ma (see below) in the Homestake area. The top of the Smithers Formation in the map area is defined as the first occurrence of pale-weathering tuff beds in the unnamed volcano-sedimentary unit. The contact is

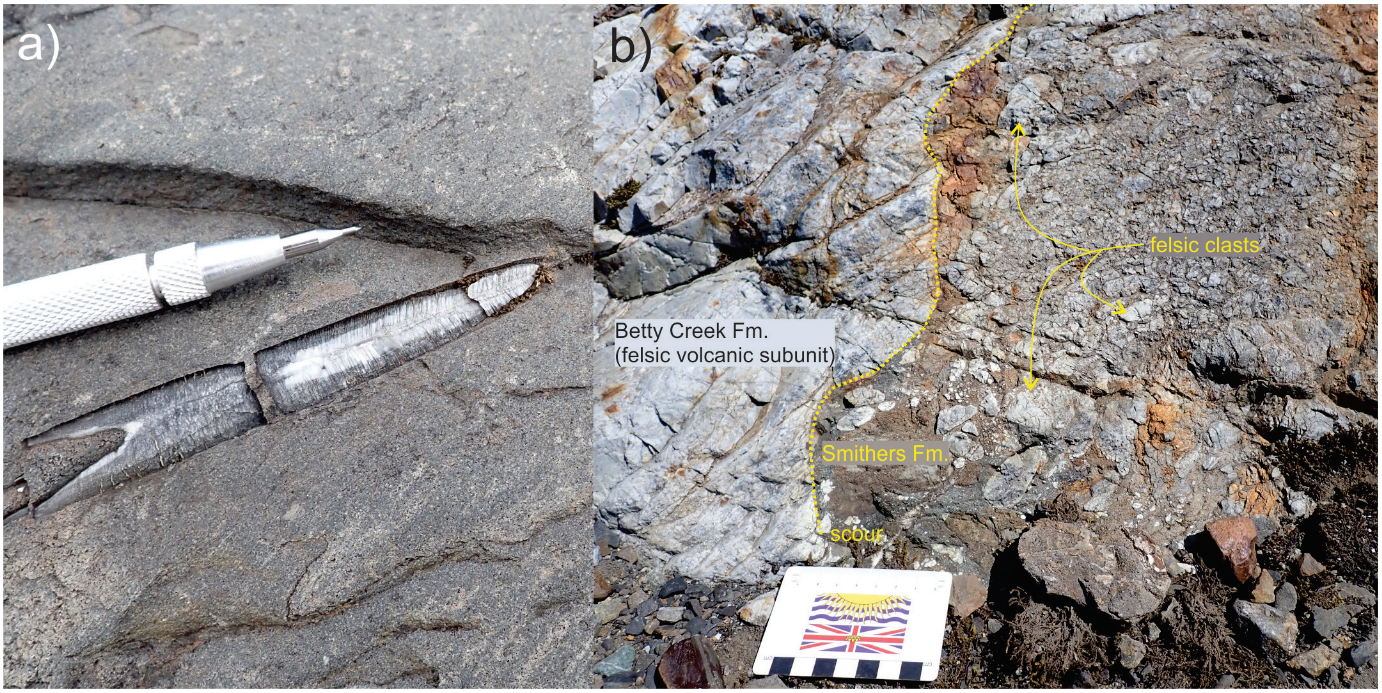

Fig. 18. Smithers Formation. **a)** Belemnite in a fine- to medium-grained massive sandstone. Taken facing N at 55.803893°N, 129.476272°W. **b)** Erosional scour between Smithers Formation clast-supported pebble to cobble conglomerate and felsic subunit of the Betty Creek Formation. Clasts of the conglomerate are predominantly the same lithology as the underlying Betty Creek Formation felsic subunit. Taken facing NE at 55.771412°N, 129.581500°W.

interpreted as conformable based on similar fossil assemblages and concordant bedding.

3.2.4.4. Unnamed volcano-sedimentary unit (Upper Jurassic)

A volcano-sedimentary unit (Upper Jurassic) is found along the flanks of the Mount McGuire anticline (Fig. 3) on the eastern, northern and western margins of the map area. It comprises well-stratified, laminated to thinly bedded mudstone, siltstone, feldspathic wacke, limestone, and rare pebbly sandstone to conglomerate interstratified with pale-weathering fine tuff to rare lapilli-tuff beds 3-20 cm thick (Fig. 19). Limestone commonly forms discontinuous elliptical to circular pods along bedding horizons. Mudstone is commonly siliceous to locally graphitic or carbonaceous. Samples from tuff layers near the base of the unit returned similar Upper Jurassic U-Pb zircon ages in the Homestake area (159.901 ±0.049 Ma) and Ajax area (157.85 ±0.033 Ma), and detrital zircon samples returned U-Pb maximum depositional ages of ca. ≤160.5 Ma (see below). The unit conformably overlies the Smithers Formation based on interstratified tuff and fossiliferous sandstone, mudstone, and limestone at Homestake Ridge, northeast of Illy, west of White Lake, and at Surebet ridge. We mapped the base of the unit as the first tuff bed above Smithers Formation fossiliferous sandstone, similar to how Gagnon et al. (2012) defined the base of the broadly coeval, but characteristically finer-grained, Quock Formation, and the top of the unit last observed tuff bed beneath overlying Bowser Lake Group siliciclastic rocks.

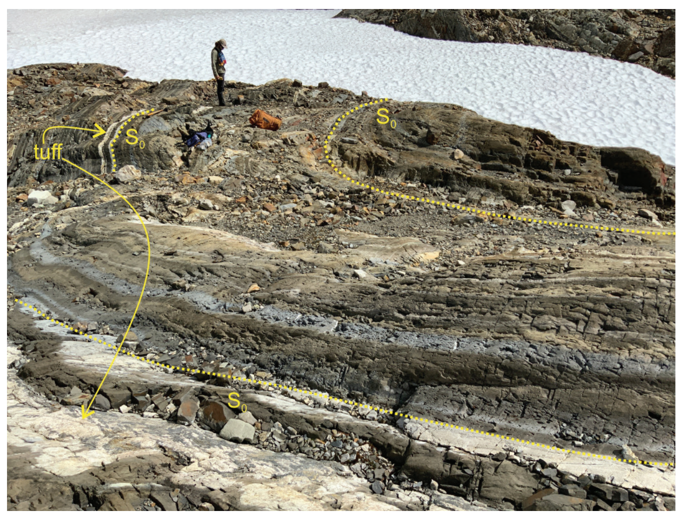

Fig. 19. Unnamed volcano-sedimentary unit. Folded interstratified siltstone, sandstone, limestone and light-weathering tuff beds. Taken facing NE at 55.612759°N, 129.679048°W.

3.3. Bowser Lake Group (Upper Jurassic)

The Bowser Lake Group bounds the map area to the north, east and south. The unit comprises grey to brown, well-stratified feldspathic wacke, siltstone, and mudstone with lesser very thick conglomerate beds locally containing chert granules and pebbles in a coarse sandstone matrix (154.3 ±0.9 Ma U-Pb detrital zircon maximum depositional age, Hunter et al., 2022a, b). Load casts, flame structures, cross bedding (Fig. 20), and mudstone intraclasts are common. The Bowser Lake Group conformably overlies the upper part of the Hazelton Group based on the concordance of bedding and lack of sub-Bowser erosional structures.

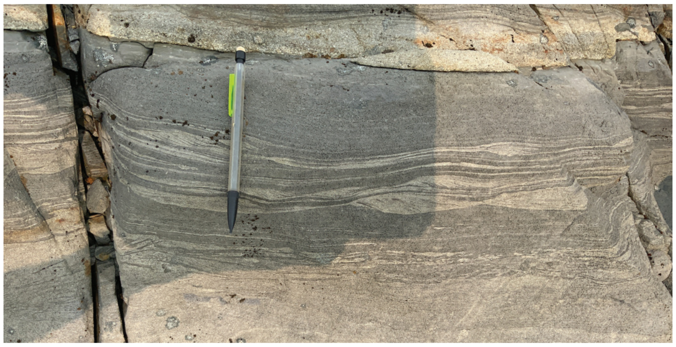

Fig. 20. Fine- to medium-grained sandstone and siltstone, Bowser Lake Group with starved ripple cross-stratification. Taken facing NE at 55.59042°N, 129.668486°W.

3.4. Eocene or younger intrusions

3.4.1. Alice Arm plutonic suite (Eocene)

Several 0.2-1.5 km^2 stocks of felsite and granite are assigned to the Alice Arm plutonic suite of MacIntyre et al. (1994). In the map area the intrusions are medium- to coarse-grained, equigranular to feldspar-quartz porphyritic, biotite-bearing granite and fine-grained biotite-bearing felsite. Stocks of the suite are associated with porphyry Mo systems such as Tidewater, Ajax, and Bell Moly (Fig. 4), and the Kitsault deposit immediately south of the map area. The granite stock that hosts the Ajax porphyry Mo system returned a U-Pb zircon crystallization age of 55.4730 ±0.0096 Ma (see below, Fig. 21).

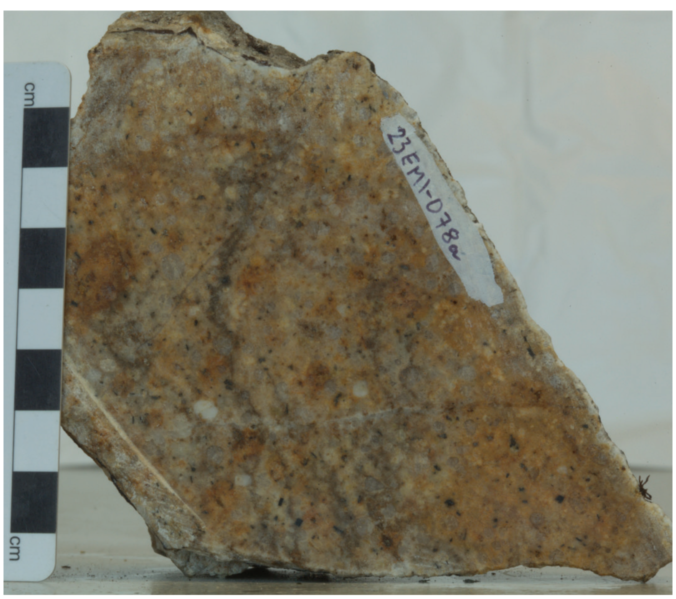

Fig. 21. Ajax stock, Alice Arm plutonic suite quartz-plagioclase-K-feldspar-phyric granite. Geochronology sample 13 (23API-84a). Collected at 55.585978°N, 129.409013°W.

3.4.2. Hyder plutonic suite (Eocene)

A large intrusive body encompasses the entire southwest corner of the map area and together with common dikes and sills are assigned here to the Hyder plutonic suite. The Hyder pluton is a coarse-grained, equigranular biotite-hornblende granodiorite to quartz monzonite (Fig. 22; ca. 61.0-51.8 Ma; Evenchick et al., 2008b; see below). It cuts rocks of the upper Hazelton Group and the Bulldog Creek pluton (Fig. 4). The dikes and sills are particularly abundant close to the margins of the Hyder pluton, where they can locally constitute more than 50% of the rock exposure and are up to 30 m wide. They display a wide range of compositions and textures from equigranular to finely porphyritic gabbro to monzonite and granodiorite. The intrusions are generally distinguishable from the earlier Texas Creek plutonic suite as they are unaffected by most deformation, except late brittle strike-slip faults and regional alteration and greenschist facies metamorphism. They cut all stratified rocks observed in the map area.

Fig. 22. Hyder pluton, coarse-grained diorite with a finer grained granodiorite xenolith and small aplite dike cutting (105°/70°). Taken facing W at 55.533144°N, 129.558148°W.

3.4.3. Lamphrophyre dikes (Eocene or younger)

A few biotite-magnetite-rich lamprophyre dikes may be similar to those that returned ca. 36.5-34.4 Ma K-Ar cooling ages (Carter, 1981).

4. Geochronology

4.1. Analytical procedures

Below we summarize the results from 12 high-precision chemical abrasion isotope dilution thermal ionization mass spectrometry (CA-TIMS) U-Pb zircon analyses, and two laser ablation inductively coupled plasma mass spectrometry (LA-ICPMS) U-Pb detrital zircon analyses (Table 2). Detailed methods and results are reported in Miller et al. (2025).

U-Pb zircon analyses were carried out at the Pacific Centre

Table 2. Summary of new geochronological ages.

Sample	No.	Age (Ma)	Type	Lithostratigraphic unit	Longitude*	Latitude*
22BvS-90b	1	204.526 ±0.037	CA-TIMS	Betty Creek Formation (lJHBvf)	-129.250803	55.642161
22EMI-001	2	193.297 ±0.035	CA-TIMS	Betty Creek Formation (lJHBvf)	-129.505119	55.688245
22RHU-77b	3	192.491 ±0.034	CA-TIMS	Betty Creek Formation (lJHBvf)	-129.334361	55.615201
23EMI-1a	4	192.079 ±0.030	CA-TIMS	Betty Creek Formation (lJHBvm)	-129.580598	55.766697
23BVA-81a	5	190.776 ±0.030	CA-TIMS	Betty Creek Formation (uTrlJHBva)	-129.592312	55.761304
22EMI-002	6	190.524 ±0.037	CA-TIMS	Betty Creek Formation (uTrlJHBva)	-129.540176	55.698519
23BVA-4a	7	190.036 ±0.032	CA-TIMS	Betty Creek Formation (lJHBvf)	-129.603287	55.780983
23API-84a	8	193.820 ±0.027	CA-TIMS	Texas Creek plutonic suite (EJTBgd)	-129.688536	55.688184
23BVA-54a	9	160.5 ±1.3	LA-ICPMS (detrital)	Unnamed volcanosedimentary unit (muJHsv)	-129.651902	55.619321
23EMI-67a	10	159.901 ±0.049	CA-TIMS	Unnamed volcanosedimentary unit (muJHsv)	-129.581395	55.775841
23EMI-134a	11	157.850 ±0.033	CA-TIMS	Unnamed volcanosedimentary unit (muJHsv)	-129.214045	55.587519
22RHU-42b	12	157.7 ±1.1	LA-ICPMS (detrital)	Unnamed volcanosedimentary unit (muJHsv)	-129.255097	55.695461
23EMI-78a	13	55.473 ±0.0096	CA-TIMS	Alice Arm plutonic suite (EAgg)	-129.409013	55.585978
23MFE-94a	14	51.8950 ±0.0099	CA-TIMS	Hyder plutonic suite (EHgd)	-129.691138	55.609981

*Datum used for all coordinates: WGS 1984

for Isotopic and Geochemical Research (University of British Columbia). Standard concordia diagrams were constructed and weighted averages calculated with Isoplot (Ludwig, 2003; Ludwig, 2012). Grains selected for CA-TIMS analysis were chosen as the youngest statistically significant population of six zircon grains with minimal inclusions and minimal rounding. For all LA-ICPMS U-Pb detrital zircon analyses we excluded individual grain ages with <0.05 probability of concordance (calculated using IsoplotR, Vermeesch, 2018). We calculated the following maximum depositional ages: youngest graphical probability peak (YPP; Dickinson and Gehrels, 2009) formed by three or more concordant grains in a probability density plot (PDP) constructed in Isoplot (Ludwig, 2012); youngest statistical population (YSP; Coutts et al., 2019); and maximum likelihood age (MLA, Vermeesch, 2021).We used the youngest statistical population as the interpreted maximum depositional age for both samples following the methods of Herriott et al. (2019).

4.2. Results

4.2.1. Betty Creek Formation

4.2.1.1. Sample 1: 22BvS-90b, andesitic lapilli-tuff

This sample was collected from the summit of a steep ridge 4.4 km east of Lavender Peak, 7.3 km east of the Big Bulk porphyry Cu-Au system (Fig. 3). It was collected at the top of the andesitic volcanic subunit near its contact with the overlying tuffaceous sedimentary subunit. The sample is a friable, maroon lapilli-tuff. Clasts in the rock are largely aphyric, they are maroon, cream, and black. Petrographic analysis shows crystal fragments include 3-5% quartz (<1 mm) and <1% white mica (<1 mm). Quartz-sericite-chlorite preferentially alters amphibole or plagioclase (<1 mm). Sixty-four grains were analyzed by LA-ICPMS. Six grains were selected for CA-TIMS analysis. Five grains mutually overlap on a concordia diagram and yield a weighted mean $^{206}Pb/^{238}U$ date of 204.526 ±0.037 Ma, which is interpreted as the crystallization age (Fig. 23). One older grain (ca. 206.9 Ma) is interpreted as an antecryst or xenocryst. This age demonstrates that the volcanic rocks near the fault contact with the Smithers Formation at the eastern margin of the map area represent a relatively early portion of the Betty Creek Formation and that the Ajax area is not a simple eastward-younging sequence as implied by the map pattern (see sample 4). This is interpreted to result from stratigraphic repetition by folds and faults.

4.2.1.2. Sample 2: 22EMI-001, dacitic ash tuff

This sample was collected from a drillhole oriented at 045°, plunging 45° collared 200 m northeast of the past-producing

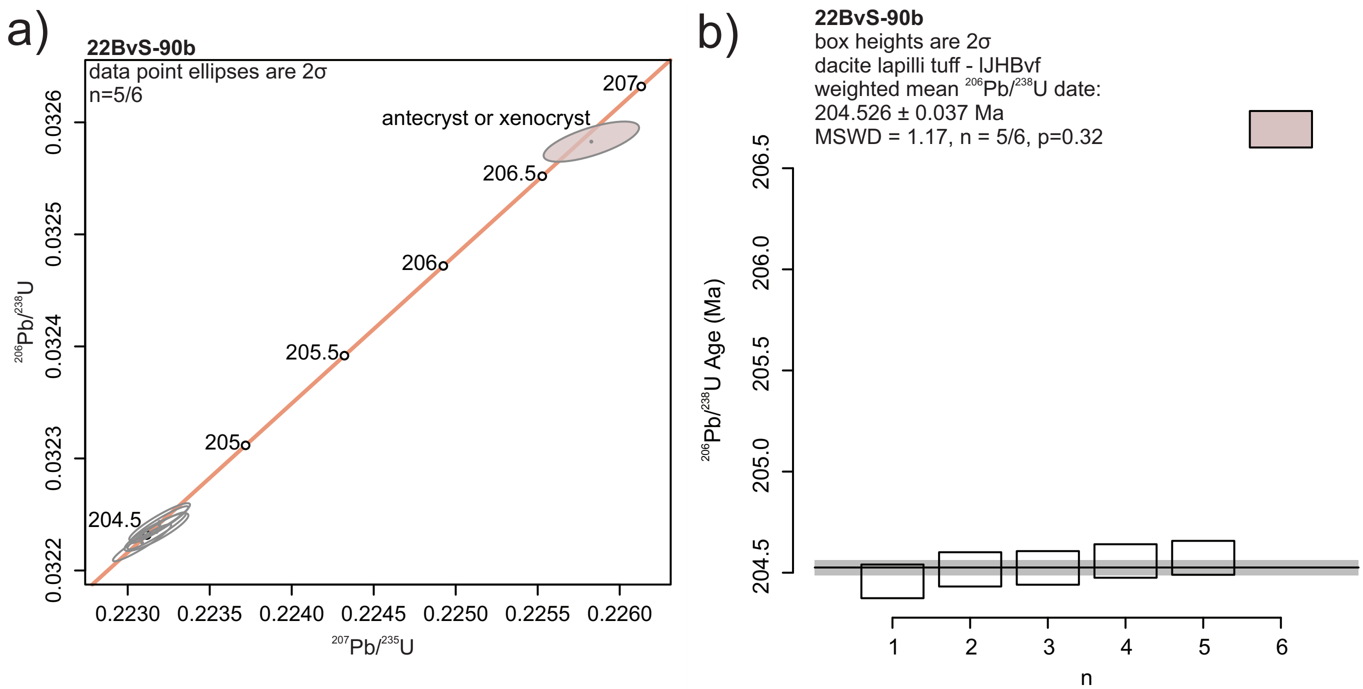

Fig. 23. CA-TIMS analyses plots of zircons, Betty Creek Formation, andesitic lapilli-tuff. **a)** Concordia plots of zircons from sample 22BvS-90b. **b)** ^{206}Pb/^{238}U ages and calculated mean age. Mean (black line), uncertainty on calculated mean (grey bar).

Torbrit mine (Fig. 3), at a downhole depth of 139 m. The sample is of a dacitic tuff from felsic subunit of the Betty Creek Formation. The sample lies 23.4 m below a zone of hydrothermal veins and breccia of jasper, sphalerite, galena, and sulfosalts, similar to mineralization at the nearby Torbrit mine. A small (<1 m) fault zone is reported in Dolly Varden drill logs between the mineralized section and the sample and, although there is no appreciable lithology change across the fault, the amount of displacement is unclear (A. Bennett, personal comm., July 2024). The sample displays moderate but pervasive sericite-chlorite-quartz alteration. Sixty-four grains were analyzed by LA-ICPMS. Six grains were selected for CA-TIMS analysis. All six analyzed grains mutually overlap on a concordia diagram and yield a weighted mean ^{206}Pb/^{238}U date of 193.297 ±0.035 Ma, which is interpreted as the crystallization age (Fig. 24). This suggests that Torbrit may be at least partially hosted in the Betty Creek Formation and limits the thickness of any overlying Kitsault unit in this part of the valley.

4.2.1.3. Sample 3: 22RHU-77b, rhyolitic lapilli-tuff to crystal tuff

This sample was collected on an unnamed peak 4.4 km south of Lavender Peak (Fig. 3). It is of a rhyolitic lapilli-tuff to crystal tuff from the andesitic volcanic subunit. Taken from an area of laminated to thickly bedded crystal tuff and tuff with minor fine lapilli-tuff, the sample contains maroon, green, tan, and grey aphyric lapilli. Petrographic analysis shows 5-10% fresh, rounded to angular quartz, plagioclase, and K-feldspar crystal fragments (0.75 mm) in a strongly and pervasively sericite- and quartz-altered ash matrix. Fifty-nine zircons were analyzed by LA-ICPMS. Six grains were selected for CA-TIMS analysis. All six analyzed grains mutually overlap on a concordia diagram and yield a weighted mean ^{206}Pb/^{238}U date of 192.491 ±0.034 Ma, which is interpreted as the crystallization age (Fig. 25). This age is considerably younger (by ca.12 Ma) than that determined for sample 1, which was collected 6 km to the west, despite the overall map pattern implying younging to the east. This is interpreted to result from folds and faults and is consistent with the observed structural contact between the Betty Creek Formation and Smithers Formation along the eastern margin rather than a continuous stratigraphic contact.

4.2.1.4. Sample 4: 23EMI-1a, andesitic tuff breccia to lapilli-tuff

This sample was collected south of the Kitsault Glacier 6.3 km west of Kitsault Lake (Fig. 3). It was collected near the top of the Betty Creek andesitic volcanic subunit 20 m stratigraphically below an unconformable contact with overlying belemnite-bearing sandstone and siltstone of the Smithers Formation (Fig. 18b). The sample is a matrix-supported tuff breccia to lapilli-tuff, with hornblende and plagioclase phenocrysts in ash- to block-sized volcanic clasts. Clasts are pale green and hornblende-phyric, maroon and amygdaloidal, and dark green, fine grained, locally plagioclase hornblende-phyric. Petrographic analysis shows 1-2% quartz grains (0.15 mm) in clasts and in the matrix, and strong calcite-chlorite-sericite±epidote alteration of all other phases, including the fine-grained matrix. Twenty zircon grains were analyzed by LA-ICPMS. Six grains were selected for CA-TIMS analysis. All six analyzed grains mutually overlap on a

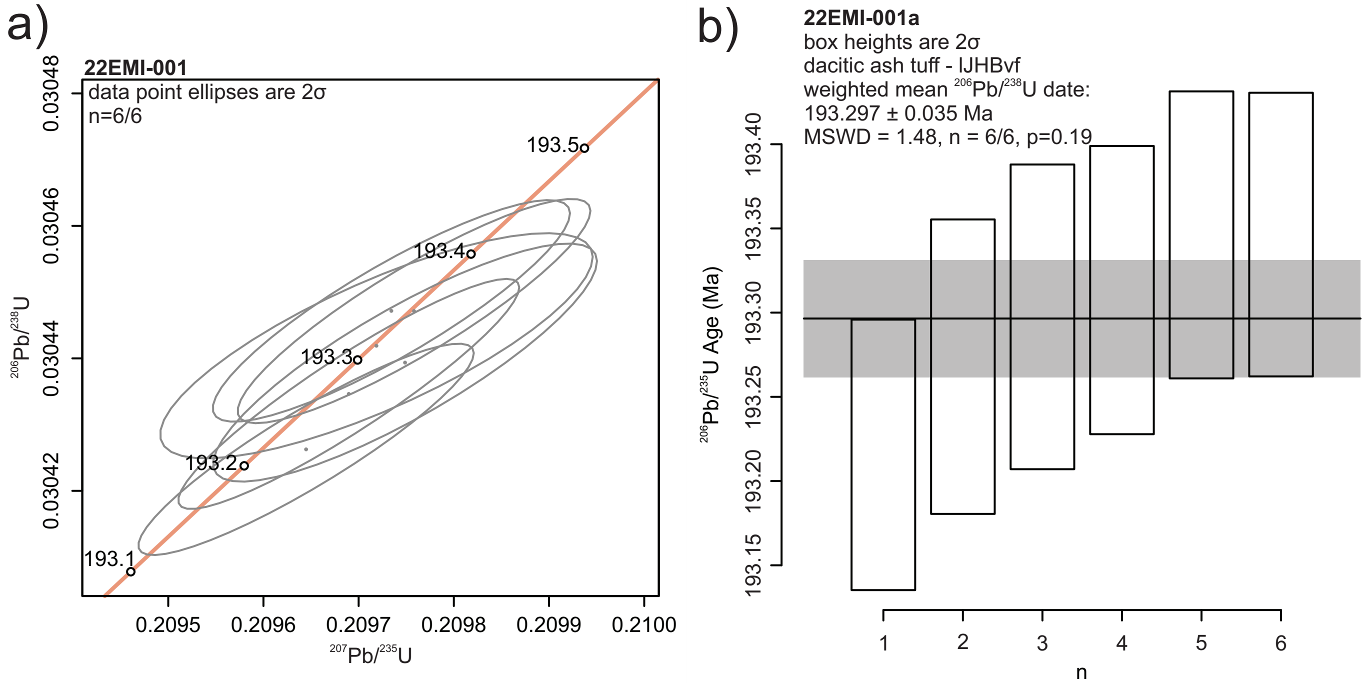

Fig. 24. CA-TIMS analyses plots of zircons, Betty Creek Formation, dacitic tuff. **a)** Concordia plot of zircons from sample 22EMI-001. **b)** $^{206}Pb/^{238}U$ ages and calculated mean age. Mean (black line), uncertainty on calculated mean (grey bar).

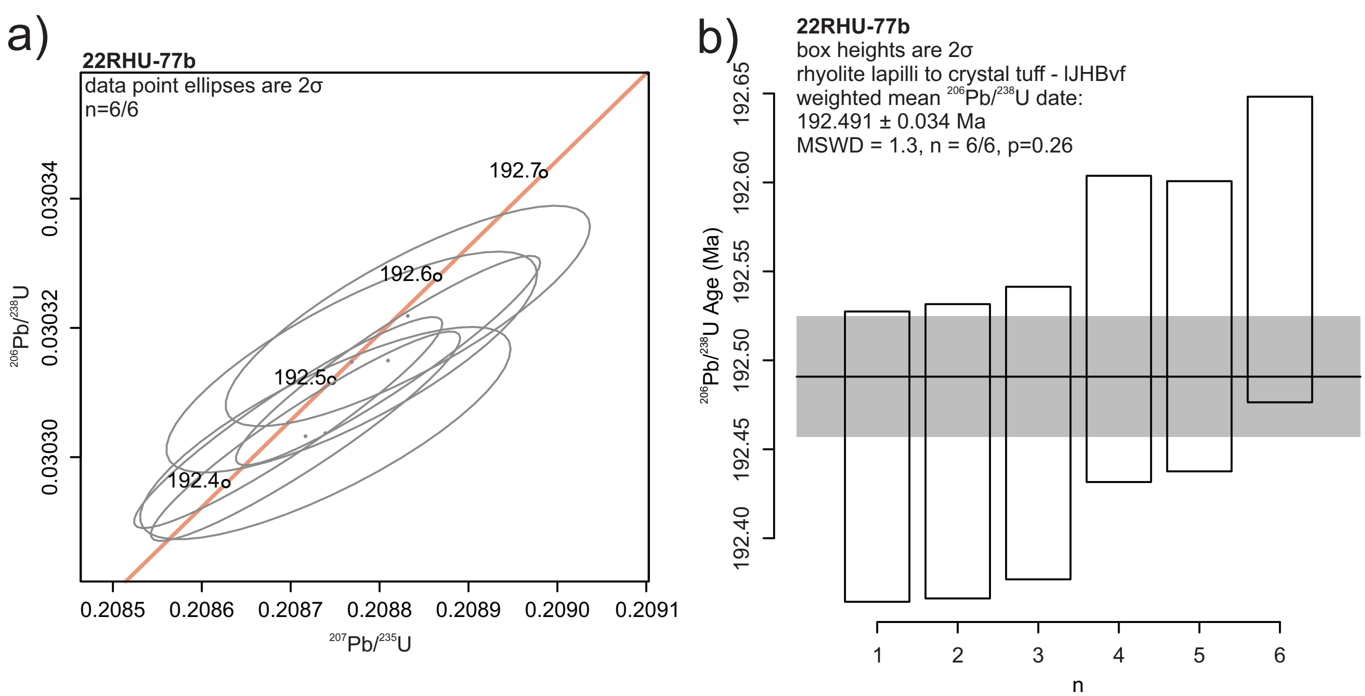

Fig. 25. CA-TIMS analyses plots of zircons, Betty Creek Formation, rhyolitic lapilli-tuff to crystal tuff. **a)** Concordia plot of zircons from sample 22RHU-77b. **b)** $^{206}Pb/^{238}U$ ages and calculated mean age. Mean (black line), uncertainty on calculated mean (grey bar).

concordia diagram and yield a weighted mean $^{206}Pb/^{238}U$ date of 192.079 ±0.030 Ma, which is interpreted as the crystallization age (Fig. 26). This age, in concert with sample 7, which was collected 2 km northwest of sample 5, confirms that the Kitsault subunit is absent in the Homestake area. Significantly older than the age determined for sample 7 from the overlying Smithers Formation (see below), this date is consistent with the interpreted sub-Smithers Formation unconformity.

4.2.1.5. Sample 5: 23BVA-81a, felsic crystal tuff to lapilli-tuff

This sample was collected from the base of the Betty Creek Formation felsic volcanic subunit above its contact with the discontinuous tuffaceous sedimentary subunit 5.4 km west of Combination Mountain, at the toe of an unnamed glacier 350 m north of the Homestake ridge deposit (Fig. 3). Petrographic analysis shows predominantly altered crystal fragments (<1 mm), with 10% subhedral fresh quartz fragments (<1 mm), and <1% euhedral to subhedral fresh plagioclase fragments (<1 mm) in a fine-grained matrix. Lapilli-sized volcanic clasts are strongly altered and contain phenocrysts of 10% subhedral quartz (<1 mm), and trace apatite and muscovite phenocrysts in a fine-grained groundmass. Calcite has altered the remaining phenocrysts, which make up 20% (<1 mm) of the lapilli. Quartz-sericite-pyrite-chlorite-calcite alteration is pervasive. Sixty-four grains were analyzed by LA-ICPMS. Six grains were selected for CA-TIMS analysis. All six grains mutually overlap on a concordia diagram and yield a weighted mean $^{206}Pb/^{238}U$ date of 190.776 ±0.030 Ma, which is interpreted as the crystallization age (Fig. 27). This age constrains the rocks hosting mineralization at Homestake ridge to Lower Jurassic.

4.2.1.6. Sample 6: 22EMI-002, andesitic crystal tuff to lapilli-tuff

This sample was collected from a drillhole collared 1.8 km east of Combination Mountain (Fig. 3), at a downhole depth of 290 m. Lapilli are rounded to sub-rounded and have well-defined margins, visible mineralogy is 20% blocky to chlorite altered hornblende fragments (1-2mm) in an ash matrix. The rock is moderately and pervasively chlorite-quartz altered. Fine-grained pyrite occurs as disseminations and in thin (1 mm) calcite-pyrite veinlets. Seventy grains were selected for LA-ICPMS analysis. Six grains were selected for CA-TIMS analysis. All six analyzed grains mutually overlap on a concordia diagram and yield a weighted mean $^{206}Pb/^{238}U$ date of 190.524 ±0.037 Ma, which is interpreted as the crystallization age (Fig. 28). This age is consistent with the interpretation of Betty Creek Formation exposure on surface.

4.2.1.7. Sample 7: 23BVA-4a, felsic tuff-breccia

This sample was collected on a ridge west of the Kitsault Glacier (Fig. 3) at the base of the felsic subunit of the Betty Creek Formation. The felsic tuff-breccia is cream coloured and contains minor white microphenocrystic clasts. Petrographic analysis shows subhedral to anhedral submillimetre crystal fragments; most are pervasively calcite-altered, with 7% fresh plagioclase, 5% quartz, and 2% K-feldspar. Coarse ash- to lapilli-sized lithic fragments contain variable amounts of <0.1 acicular plagioclase phenocrysts in a very fine-grained groundmass. Fifty-seven grains were selected for LA-ICPMS analysis. Six grains were selected for CA-TIMS analysis. All six grains mutually overlap on a concordia diagram and yield a weighted mean $^{206}Pb/^{238}U$ date of 190.036 ±0.032 Ma, which is

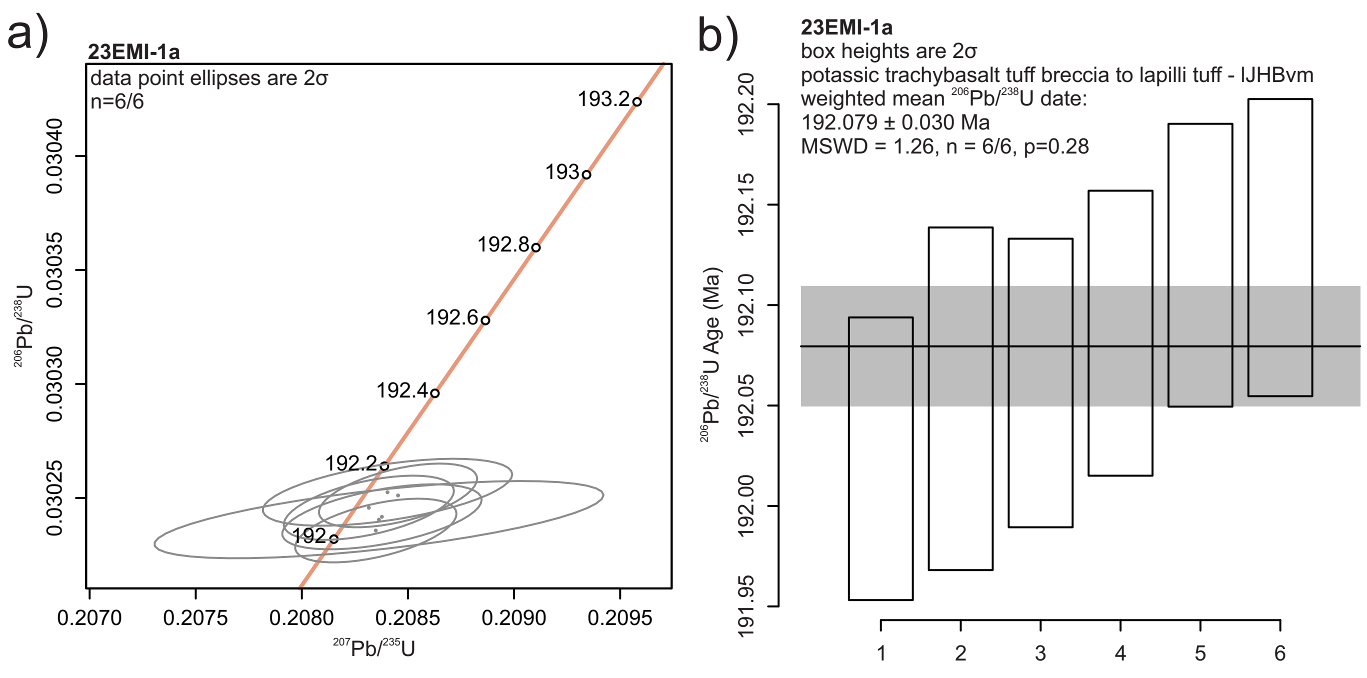

Fig. 26. CA-TIMS analyses plots of zircons, Betty Creek Formation, andesitic tuff breccia to lapilli-tuff. **a)** Concordia plot of zircons from sample 23EMI-1a. **b)** $^{206}Pb/^{238}U$ ages and calculated mean age. Mean (black line), uncertainty on calculated mean (grey bar).

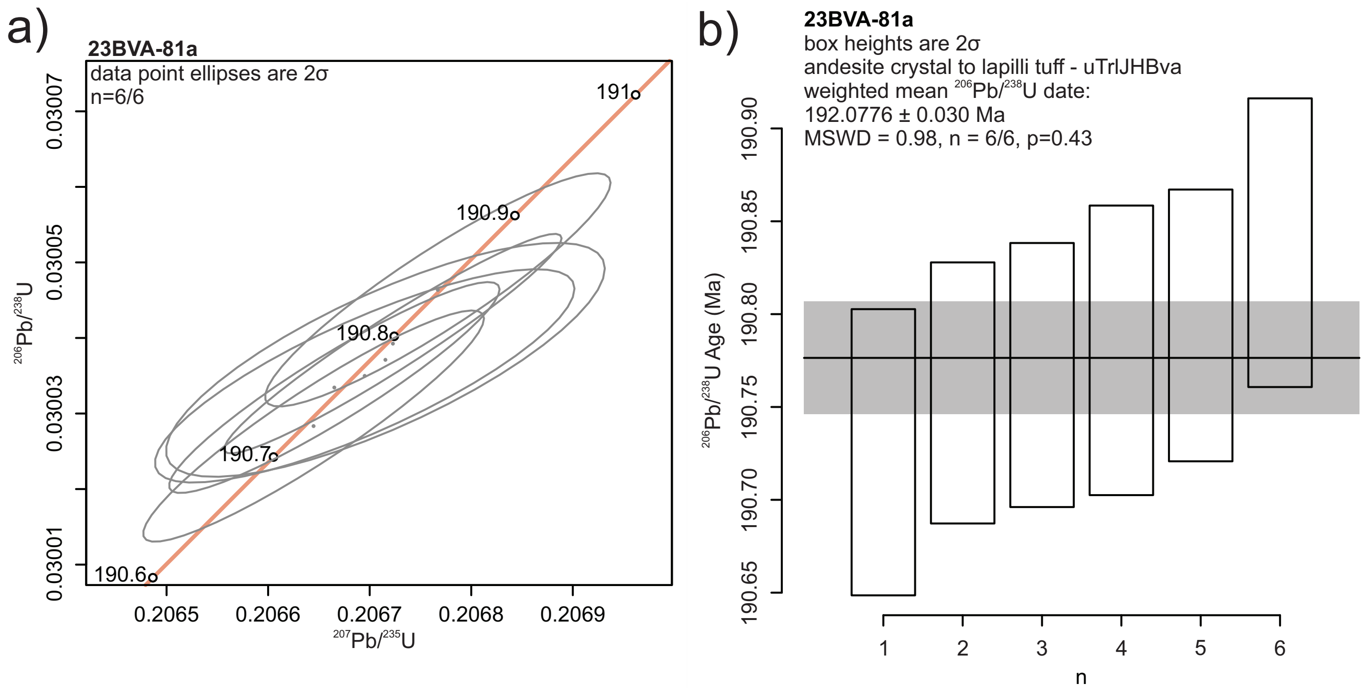

Fig. 27. CA-TIMS analyses plots of zircons, Betty Creek Formation, felsic crystal tuff to lapilli-tuff. **a)** Concordia plot of zircons from sample 23BVA-81a. **b)** $^{206}Pb/^{238}U$ ages and calculated mean age. Mean (black line), uncertainty on calculated mean (grey bar).

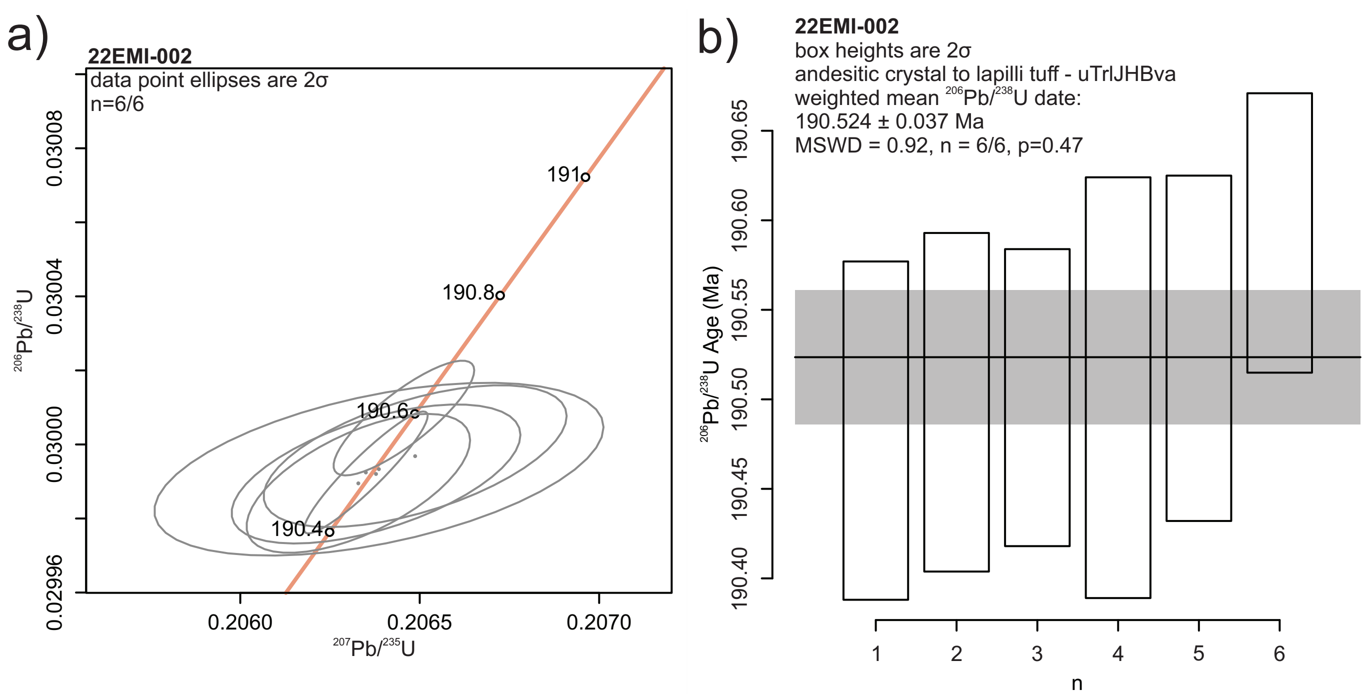

Fig. 28. CA-TIMS analyses plots of zircons, Betty Creek Formation, andesitic crystal tuff to lapilli-tuff. **a)** Concordia plot of zircons from sample 22EMI-002. **b)** $^{206}Pb/^{238}U$ ages and calculated mean age. Mean (black line), uncertainty on calculated mean (grey bar).

interpreted as the crystallization age (Fig. 29). This age, along with sample 5, is consistent with the absence of the Kitsault unit (Lower to Middle Jurassic) in this portion of the map area.

4.2.2. Texas Creek plutonic suite

4.2.2.1. Sample 8: 23API-84a, quartz monzonite

This sample was collected from the Bulldog Creek pluton 7.7 km west of the peak of Combination Mountain (Fig. 3) from a creek on the side of a steep subalpine ridge. Rocks at the sample site contain 5-10% quartz phenocrysts (2-4 mm) in an 80% feldspathic groundmass. Accessory minerals include biotite and hornblende. Petrographic analysis shows the sample contains 25% blocky, elongate to equant hornblende (<1 mm), 30% plagioclase (<1 mm), 28% K-feldspar (<1 mm), 15% subhedral quartz crystals (0.5 mm), and 2-3% entirely chlorite-replaced biotite (<1 mm). The sample is weakly and patchily quartz-chlorite-sericite altered, with sericite alteration targeting feldspars. Fifty-nine zircon grains were analyzed by LA-ICPMS. Six grains were selected for CA-TIMS analysis. All six analyzed grains mutually overlap on a concordia diagram and yield a weighted mean $^{206}Pb/^{238}U$ date of 193.820 ±0.027 Ma, which is interpreted as the crystallization age (Fig. 30). This confirms that this batholith is part of the Bulldog Creek pluton, as dated and described by Evenchick et al. (2008b), and is coeval with Betty Creek Formation. South of the sample site, the pluton cuts volcanic rocks, constraining them as Betty Creek or older and suggesting that the Kitsault unit is absent in the Surebet area.

4.2.3. Unnamed volcano-sedimentary unit

4.2.3.1. Sample 9: 23BVA-54a, volcanic-derived sandstone

This sample was collected from sedimentary rocks of the unnamed unit on Surebet ridge, west of the Varden Glacier and 1.4 km northeast of the Surebet occurrence (Fig. 3). The sample site is in an area of good to nearly continuous exposure along the ridge of interbedded siltstone, very fine-grained sandstone, and lesser tuff and limestone beds. Rare coarse-grained sandstone beds contain angular to subangular feldspar, lesser quartz, and possible chert. Petrography shows that the sample is a texturally and compositionally immature volcanic-derived feldspathic wacke containing 30% angular to rounded quartz, 10% plagioclase, trace angular to subangular K-feldspar, and trace muscovite, and in a fine-grained quartz-carbonate matrix. There is trace quartz-sericite alteration of the matrix and some feldspar grains. One hundred and ninety-seven zircon grains were analyzed by LA-ICPMS. A probability density plot of these 197 grains shows two distinct Early to Late Jurassic peaks, with the youngest significant peak at 160.5 Ma. (Fig. 31a). A younger (Early Cretaceous) population is from three grains suspected to have undergone lead loss and were not considered in analysis; 17 discordant grains were also excluded. A youngest statistical population maximum depositional age of 160.5 ±1.3 Ma was calculated from a population of 39 grains (Fig. 31b). This confirms that the maximum depositional age for rocks in the upper part of Hazelton Group in the Surebet area is similar to elsewhere in the map area and constrains the age of the rocks that host mineralization at the Surebet project. A population of Paleozoic zircon grains may record derivation from the Stikine assemblage.

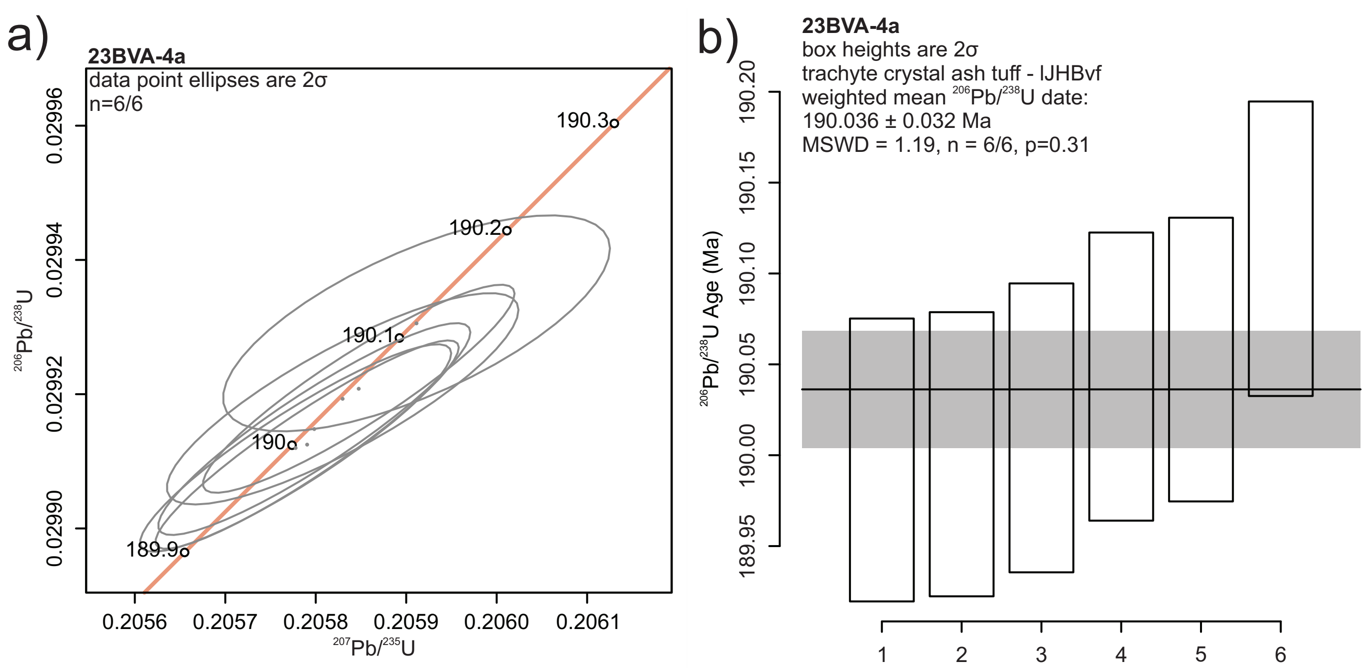

Fig. 29. CA-TIMS analyses plots of zircons, Betty Creek Formation, felsic tuff-breccia. **a)** Concordia plot of zircons from sample 23BVA-4a. **b)** $^{206}Pb/^{238}U$ ages and calculated mean age. Mean (black line), uncertainty on calculated mean (grey bar).

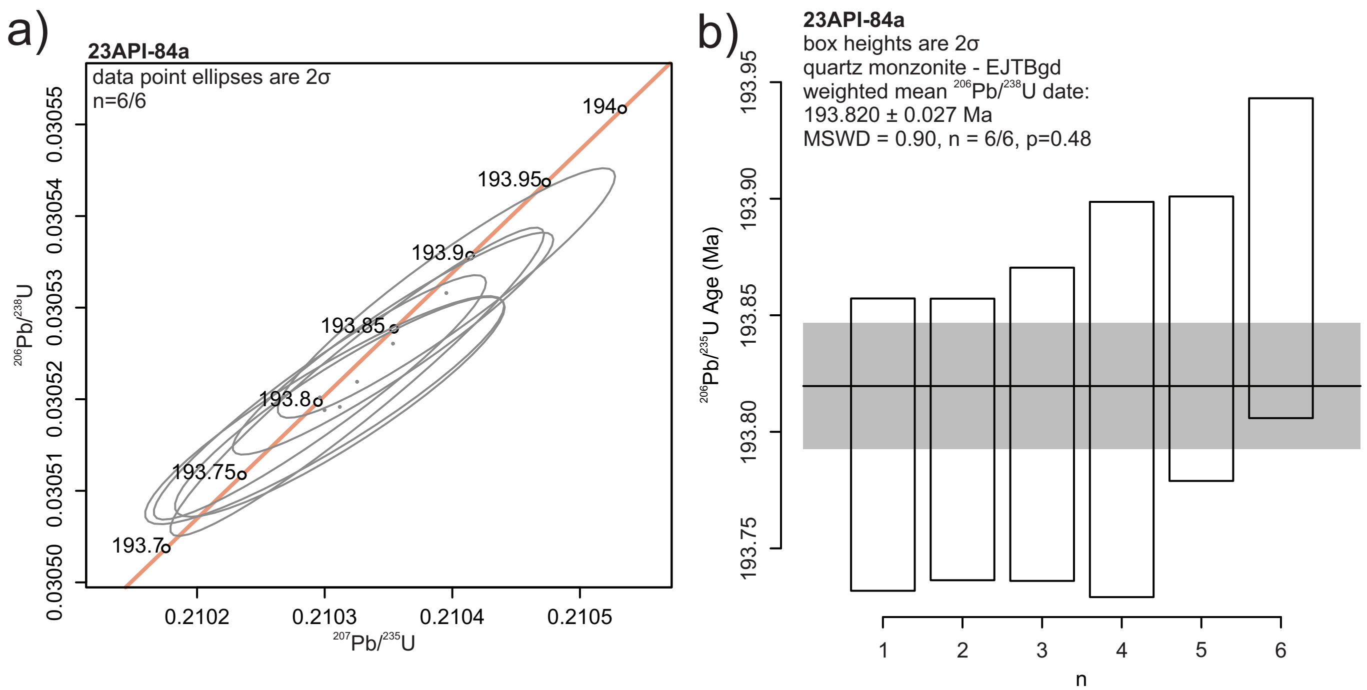

Fig. 30. CA-TIMS analyses plots of zircons, Texas Creek plutonic suite, Bulldog Creek pluton, quartz monzonite. **a)** Concordia plot of zircons from sample 23API-84a. **b)** ^{206}Pb/^{238}U ages and calculated mean age. Mean (black line), uncertainty on calculated mean (grey bar).

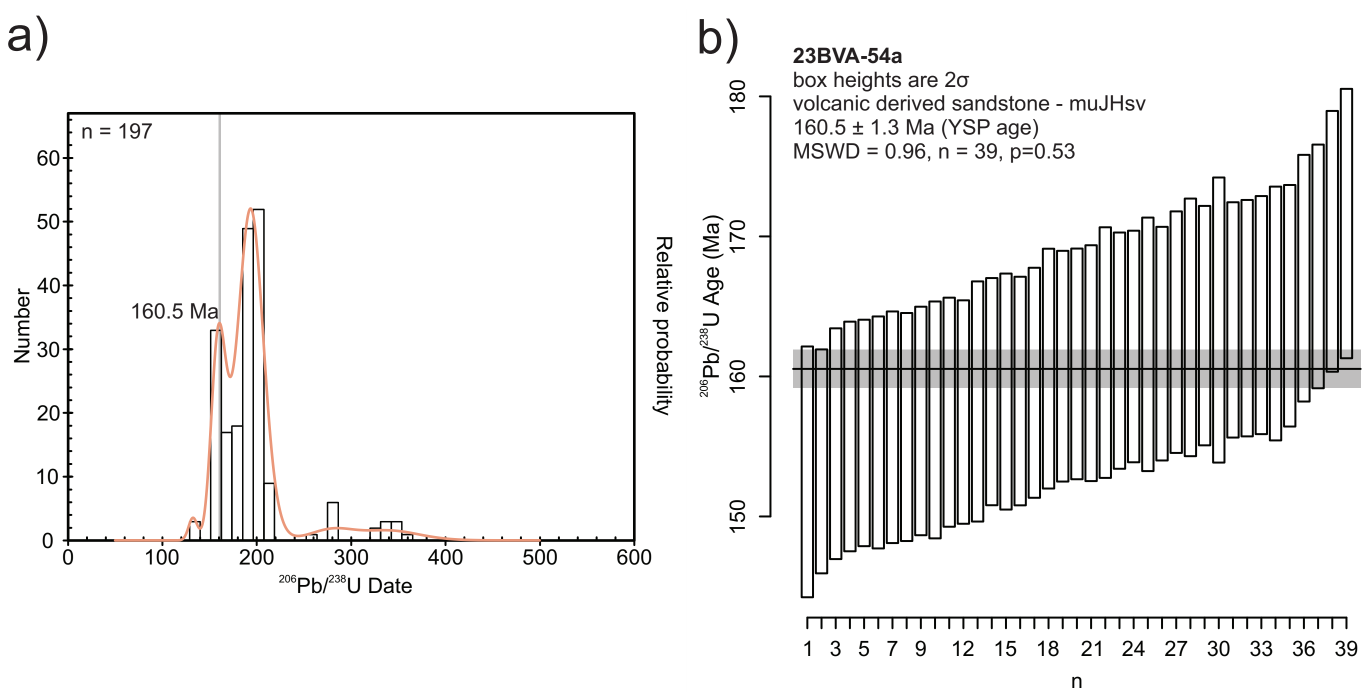

Fig. 31. LA-ICPMS analyses plots of detrital zircons, unnamed volcano-sedimentary unit, volcanic-derived sandstone. **a)** ^{206}Pb/^{238}U probability density plot showing the main probability age peaks for sample 23BVA-54a and calculated youngest statistical population (YSP) age (grey bar). **b)** ^{206}Pb/^{238}U ages and calculated mean age for the youngest statistical population.

4.2.3.2. Sample 10: 23EMI-67a, crystal tuff

This sample was collected from near the base of the unnamed volcano-sedimentary unit at the headwaters of Homestake Creek at the toe of the Kitsault Glacier, 6.5 km northwest of Kitsault Lake (Fig. 3). Recognizing bedding repetition from isoclinal folds, we sampled the first accessible tuff bed in a section with unambiguous younging; other tuff beds are lower in the section but inaccessible. Petrography indicates that the crystal tuff contains ~80% subhedral feldspar crystal fragments (0.1 mm) and ~5% quartz fragments (0.1 mm) in a fine ash matrix. The feldspar is strongly replaced by sericite and the matrix and lithic fragments are weakly to moderately altered to sericite-chlorite-calcite. Forty-five zircons were analyzed by LA-ICPMS. Six grains were selected for CA-TIMS analysis. All six grains mutually overlapped on a concordia diagram and yielded a weighted mean $^{206}Pb/^{238}U$ date of 159.901 ±0.049 Ma (Upper Jurassic) which is interpreted as the crystallization age (Fig. 32).

4.2.3.3. Sample 11: 23EMI-134a, felsic tuff

This sample was collected from the unnamed volcano-sedimentary unit in the southeast portion of the map area, in a small drainage, 2 km NE of Illiance Mountain (Fig. 3). The sample is from a white weathering felsic tuff bed in otherwise dark sedimentary rocks 380 m stratigraphically above the contact with the underlying Smithers Formation. Petrographic observation shows a fabric in the rock defined by variable proportions of ash, crystals and elongate volcanic clasts. Crystal-rich layers contain 30% rounded to subrounded plagioclase (<1 mm), 20% quartz, and <1% muscovite in a fine grained ash matrix. Crystal-poor layers are more sericite altered and composed of fine ash. The sample is moderately sericite altered throughout. Sixty-one zircon grains were analyzed by LA-ICPMS. Six grains were selected for CA-TIMS analysis. All six grains mutually overlap on a concordia diagram and yielded a weighted mean $^{206}Pb/^{238}U$ date of 157.850 ±0.033 Ma, which is interpreted as the crystallization age (Fig. 33). This confirms a Late Jurassic age for magmatism associated with this unit and indicates that the tuff beds in the unnamed volcanosedimentary unit span 2 m.y. or more of activity.

4.2.3.4. Sample 12: 22RHU-42b, subfeldspathic arenite

This detrital zircon sample was collected 6.5 km east of the northern end of Kinskuch Lake (Fig. 4), from outcrop at the end of a steep ridge consisting of finely interbedded sandstone, siltstone, and tuff. An interval of massive feldspathic sandstone was sampled for analysis. The sandstone is a weakly quartz-sericite-calcite altered volcanic-derived subfeldspathic arenite containing 70% angular quartz (<1 mm), 20% plagioclase, and 1% muscovite bonded by quartz-carbonate cement. One hundred and forty-eight zircon grains were selected for LA-ICPMS analysis. A probability density plot of these 148 grains shows two distinct Early to Late Jurassic peaks with the youngest significant peak at 158.0 Ma. (Fig. 34a). One Late Jurassic grain is suspected to have undergone lead loss and was not considered in analysis; 16 discordant grains were also excluded. A youngest statistical population maximum depositional age of 157.7 ±1.1 Ma was calculated from a population of 26 grains (Fig. 34b), consistent with a maximum depositional age from the upper part of the Hazelton Group

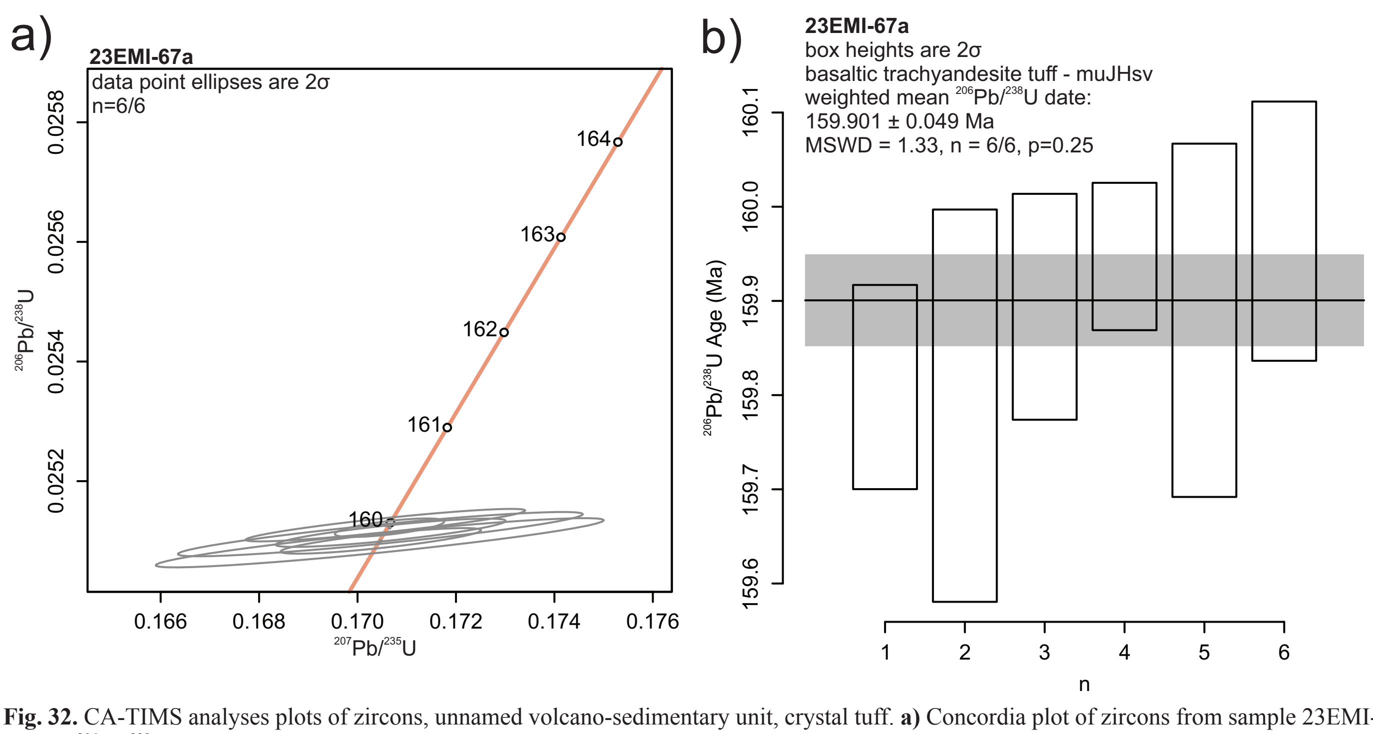

Fig. 32. CA-TIMS analyses plots of zircons, unnamed volcano-sedimentary unit, crystal tuff. **a)** Concordia plot of zircons from sample 23EMI-67a. **b)** $^{206}Pb/^{238}U$ ages and calculated mean age. Mean (black line), uncertainty on calculated mean (grey bar).

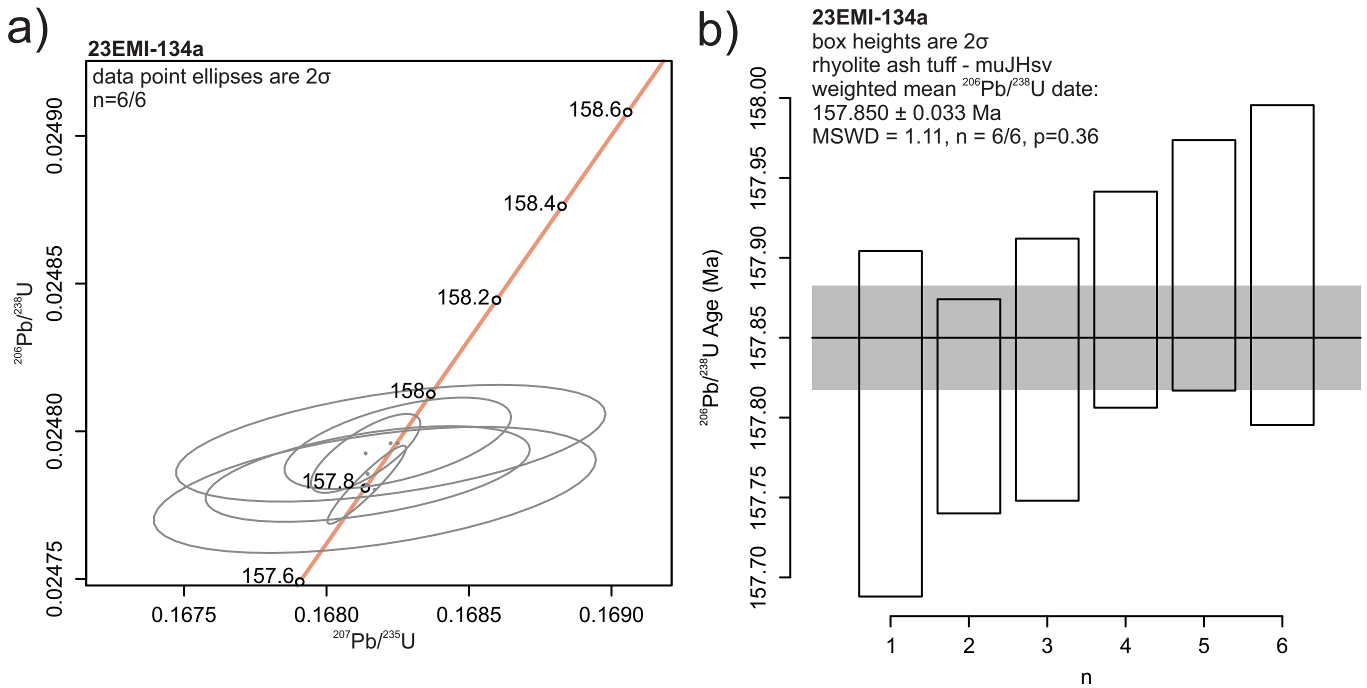

Fig. 33. CA-TIMS analyses plots of zircons, unnamed volcano-sedimentary unit, felsic tuff. **a)** Concordia plot of zircons from sample 23EMI-134a. **b)** $^{206}Pb/^{238}U$ ages and calculated mean age. Mean (black line), uncertainty on calculated mean (grey bar).

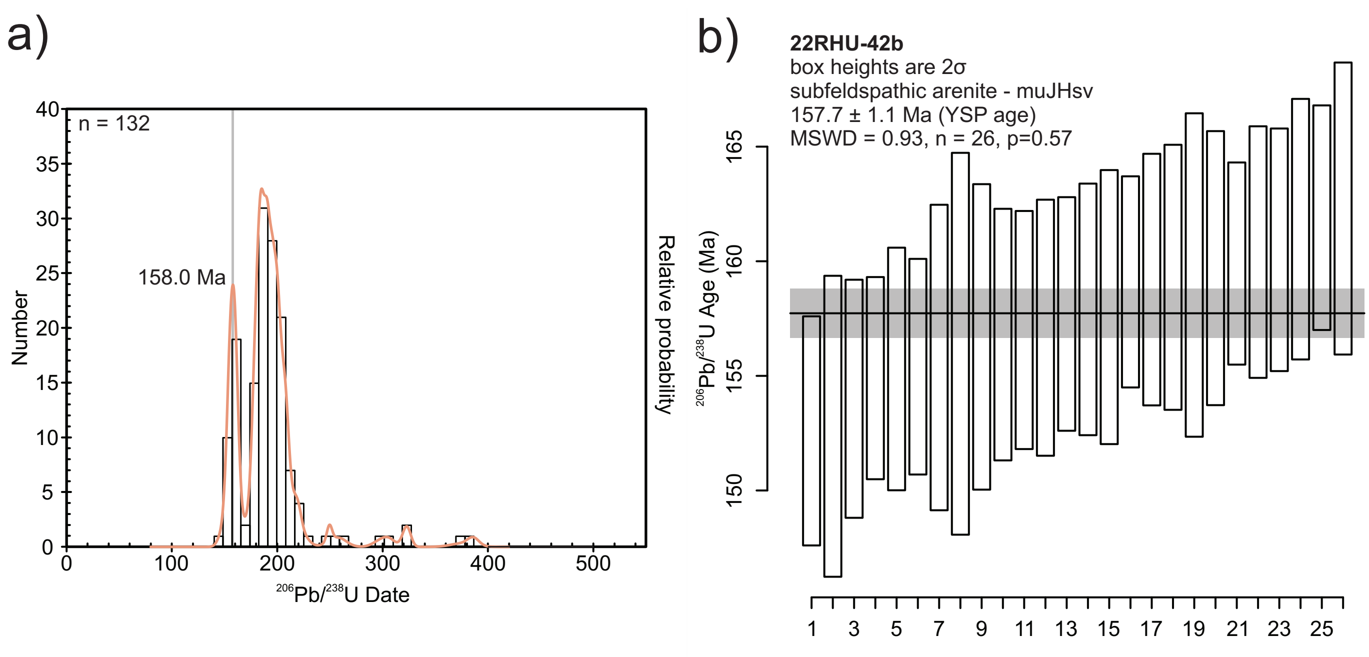

Fig. 34. LA-ICPMS analyses plots of detrital zircons, unnamed volcano-sedimentary unit, subfeldspathic arenite. **a)** $^{206}Pb/^{238}U$ probability density plot showing the main probability age peaks for sample 22RHU-42b and calculated youngest statistical population (YSP) age (grey bar). **b)** $^{206}Pb/^{238}U$ ages and calculated mean age for the youngest statistical population.

elsewhere in the map area. A population of Paleozoic zircon grains in the sample may record derivation from the Stikine assemblage.

4.2.4. Alice Arm plutonic suite
4.2.4.1. Sample 13: 23EMI-78a, granite

This sample was collected from the side of a steep ridge near the centre of the Ajax stock, 600 m west of the peak of Mount McGuire (Fig. 3), and is of a weakly chlorite-sericite-calcite altered granite. The rock is pale weathering, white on fresh surfaces, and ranged from aplitic to coarsely porphyritic. The sample contains (50%) subhedral quartz phenocrysts (1.5-2 mm), 15% locally zoned subhedral plagioclase (1-1.5 mm), and 5-10% K-feldspar in a fine-grained groundmass with subhedral quartz. Accessory minerals include muscovite (1-2%) and apatite and lesser biotite. Sixty zircon grains were analyzed be LA-ICPMS. Six grains were selected for CA-TIMS analysis. All six grains mutually overlap on concordia and yielded a weighted mean ^{206}Pb/238U age of 55.473 ±0.0096 Ma, which is interpreted as the crystallization age (Fig. 35), confirming that Ajax Mo porphyry deposit is hosted by Eocene rocks.

4.2.5. Hyder plutonic suite
4.2.5.1. Sample 14: 23MFE-94a, granodiorite

This sample was collected on a ridge near the intrusive contact between the Hyder pluton and Bowser Lake Group sedimentary rocks, 6.6 km west of Mount Klayduc (Fig. 3). The sample is of a grey-weathering, medium- to coarse-grained, equigranular granodiorite taken from a section of near continuous of exposure on top of a ridge near the edge of the pluton. The sample contains 50% euhedral to anhedral plagioclase (3.5-4 mm), 30% anhedral quartz (1.5 mm), 5-10% anhedral K-feldspar (1.5 mm), 5% biotite, and 3% amphibole. Sixty-two zircon grains were analyzed by LA-ICPMS. Six grains were selected for CA-TIMS analysis. All six grains mutually overlap on concordia and yielded a weighted mean ^{206}Pb/^{238}U age of 51.8950 ±0.0099 Ma, which is interpreted as the crystallization age (Fig. 36).

5. Discussion: implications for the geological setting and distribution of mineral deposits in the Kitsault River area

New U-Pb zircon geochronology and the updated geological map provide a framework for understanding the stratigraphic and structural setting of the Hazelton Group and distribution of latest Triassic to Eocene mineral deposits in the Kitsault River area and provides insights into regional tectonic episodes that shaped its geological history. Mineralization can be divided into three metallogenic events separated by tectonic shifts marked by unconformities and deformation: 1) latest Triassic to Jurassic porphyry Cu-Au and epithermal deposits hosted in and coeval with the lower part of the Hazelton Group and Texas Creek plutonic suite; 2) late Early Jurassic to Middle Jurassic VMS and epithermal deposits hosted in and coeval with the upper part of the Hazelton Group; 3) Eocene Mo porphyry systems associated with the Alice Arm plutonic suite, and fault-hosted Au-Ag mineralization.

5.1. Stuhini to lower Hazelton Group transition (latest Triassic)

The Kinskuch unit (latest Triassic; Rhaetian) is more extensive than previously recognized. In addition to the Big Bulk area where it was first defined (Miller et al., 2020) the unit is locally

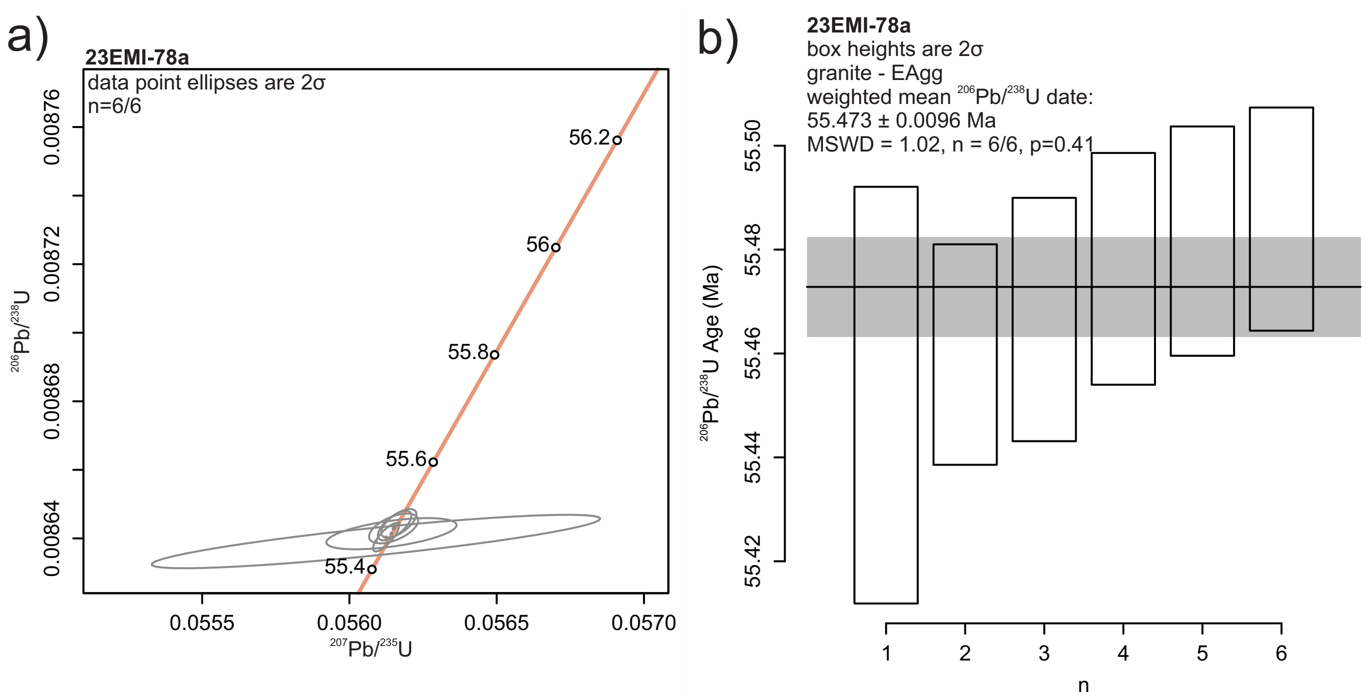

Fig. 35. CA-TIMS analyses plots of zircons, Alice Arm plutonic suite, Ajax stock, granite. **a)** Concordia plot of zircons from sample 23EMI-78a. **b)** ^{206}Pb/^{238}U ages and calculated mean age. Mean (black line), uncertainty on calculated mean (grey bar).

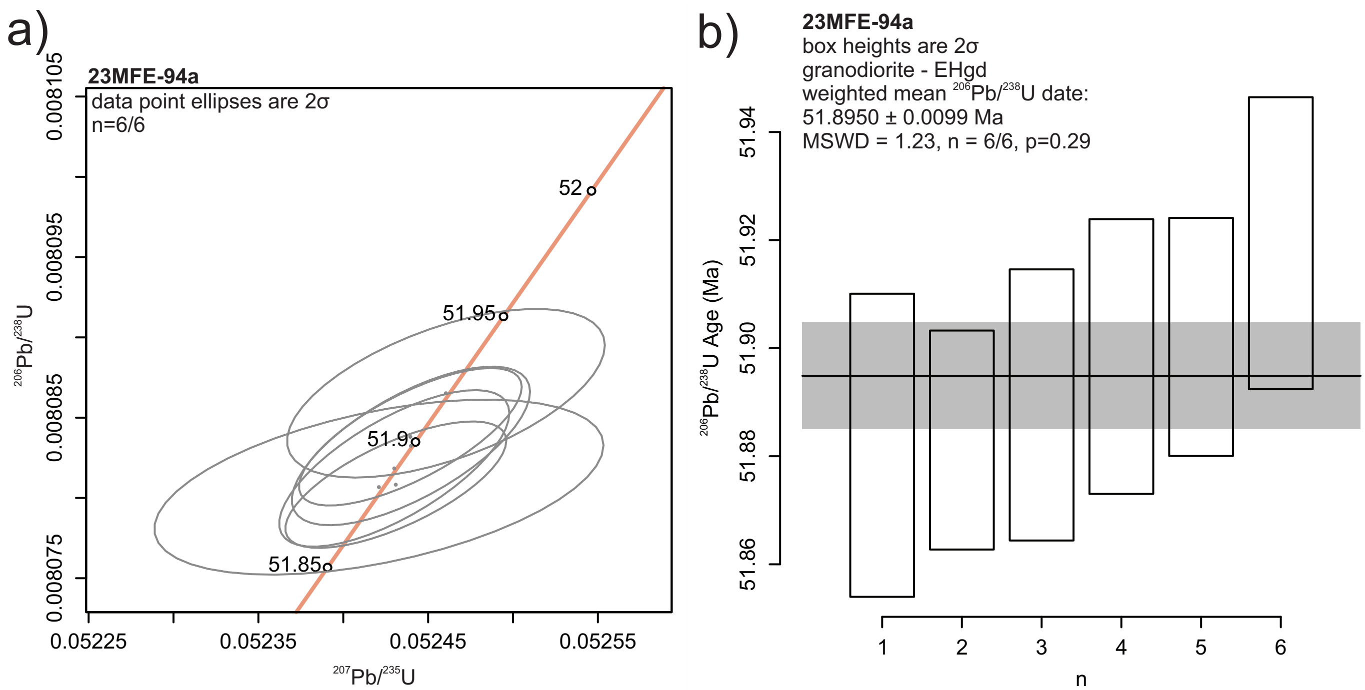

Fig. 36. CA-TIMS analyses plots of zircons, Hyder plutonic suite, granodiorite. **a)** Concordia plot of zircons from sample 23MFE-94a. **b)** $^{206}Pb/^{238}U$ ages and calculated mean age. Mean (black line), uncertainty on calculated mean (grey bar).

at the base of the Hazelton Group in the Homestake and Surebet areas (Fig. 3). The unit records significant paleotopography, a necessity for the generation and preservation of the locally (up to >320 m) thick conglomerates and deep incision into underlying strata (at least as deep as basement Stikine assemblage) indicated by the clast compositions, and a component of dip-slip motion along syn-sedimentary faults. The absence of Kinskuch unit between Stuhini Group sedimentary rocks and Hazelton Group volcanic rocks, which are in conformable contact southwest of Jade Lake, demonstrates that the uneven distribution of the unit cannot be completely explained due to loss via later erosion but is at least partially due to development of local fault-controlled sub-basins. The intraformational volcanic clasts within the Kinskuch unit record early Hazelton Group volcanism in the region. Although lacking in significant quartz-rich detritus, which reflects the absence of Stikine plutonic suite intrusions or other quartz-bearing units in the source region, the Kinskuch unit is the stratigraphic equivalent to the Jack Formation exposed in the Iskut River area, also likely controlled by syn-depositional faults (Nelson et al., 2018, 2022).

5.2. Lower Hazelton Group and Texas Creek plutonic suite magmatism and mineralization (latest Triassic to Early Jurassic)

The lower part of the Hazelton Group records a period of prolific volcanism (latest Triassic to Early Jurassic, ca. ≤206-190 Ma. The new geochronology and fieldwork confirm that Betty Creek Formation subunits overlap in age and grade laterally into one another. This demonstrates that, although overall character was largely andesitic as described historically (Alldrick et al., 1986; Dawson and Alldrick, 1986; Evenchick, 2001), magmatic composition varied between eruptive events and/or volcanic centres. Some augite-phyric basalts, which are characteristic of the Stuhini Group (Late Triassic), are now considered consistent with inclusion in the Betty Creek Formation. Significant paleotopography (Fig. 6) likely persisted locally through the Early Jurassic.

Stocks of the Texas Creek plutonic suite in the map area (latest Triassic to Early Jurassic, ca. 204.6-191.7 Ma) are coeval with, and almost perfectly overlap in age with the Betty Creek Formation, suggesting eruptive volcanism was active throughout the entire lower Jurassic magmatic event. Texas Creek plutonic suite rocks cut the Stuhini Group, Kinskuch unit, and Betty Creek Formation, and host and/or are considered coeval with mineralization at several showings including the Big Bulk porphyry Au-Cu system and the Homestake Au-Ag-Cu epithermal deposit (Fig. 3).

The Homestake deposit is hosted in Stuhini Group and lower Hazelton Group rocks cut by abundant monzonite to diorite stocks and dikes (Early Jurassic; ca. 191.7 Ma; Hunter and van Straaten, 2020). The intrusions are likely coeval with vein and breccia-hosted Au-Ag-Cu mineralization and span the timing of alteration (Swanton et al., 2013). Our revised mapping supports the interpretation that mineralization is Early Jurassic or younger. The presence of Kinskuch unit and significant northerly- and easterly-trending faults close to the Homestake deposit suggests the possibility of emplacement into a local latest Triassic fault-controlled basin similar to that proposed for the Big Bulk system.

5.3. Upper Hazelton Group magmatism and mineralization (late Early Jurassic to Middle Jurassic)

Our mapping has recognized a 15 km-long belt of felsic, intermediate, and mafic volcanic rocks assigned to the Kitsault unit (upper part of the Hazelton Group) in the northern part of the study area on the western limb and axial surface trace of the Mount McGuire anticline. It is distinguished from the Betty Creek Formation based on geochronology and stratigraphic position above a thin package (10-100 m) of locally exhalative-bearing (e.g., Sault Zn-Pb-Ag-Sr showing; Fig. 3) sedimentary rocks assigned to the Spatsizi Formation (ca. ≤188 Ma; Hunter et al., 2022). Geochronology suggests a Lower to Middle Jurassic age (ca. ≤188 to ≤168 Ma) for this unit.

The Dolly Varden deposits are near the confluence of the surface expression of the Kitsault unit and the branching termination of the north northeast-trending Kitsault River fault and its secondary structures (Fig. 3; Devlin and Godwin, 1986; McCuaig and Sebert, 2017). These faults are likely part of a syn-sedimentary network related to the long-lived (latest Triassic or older) faults identified at the Kinskuch Lake area. It is likely that these faults provided pathways for mineralizing fluids produced during Kitsault unit volcanism, which is consistent with the presence of fault-hosted mineralization described by Sebert and Ramsay (2012) at the Wolf deposit.

The Wolf deposit is hosted in ca. 178 Ma or younger tuffaceous rocks (Hunter et al., 2022c), and includes crosscutting (i.e., fault controlled, veins and breccias) as well as syngenetic mineralization (i.e., clastic sulphides, and altered and mineralized clasts; Sebert and Ramsay, 2012), the latter of which suggests mineralization is of a similar age to the host rocks. The other Dolly Varden deposits (including Dolly Varden, Torbrit, and North Star) are interpreted as coeval with the Wolf deposit on the basis of similar mineralogical and textural characteristics (Hunter and van Straaten, 2020 and references therein). The dacitic tuff from a drill hole that returned an age of ca. 193 Ma (sample 2), suggests that the Torbrit deposit could be hosted by the Betty Creek Formation but we have maintained the field interpretation of exposures near this drill hole as Kitsault unit volcanic rocks, pending results from additional surface geochronological samples.

The Kitsault unit is roughly coeval to other post-arc, syn-collisional magmatism recognized in the upper part of Hazelton Group such the Horn Mountain Formation (ca. 185-171 Ma; van Straaten et al., 2022; van Straaten, 2024) of the Stikine arch, the rift-related rocks of the Iskut River Formation (ca. 179-173 Ma; Nelson et al., 2018, and references therein), and the rift-proximal Mount Dilworth Formation in the Stewart area (ca. 173.6, Cutts et al., 2015; Alldrick, 1993). The Kitsault unit is east of the main Eskay rift trend (Fig. 2) and lacks the distinctly bimodal volcanism and rhyolites characteristic of the Iskut River Formation. It more closely resembles the arc-like volcanic rocks of the Horn Mountain Formation, which comprises mafic, and intermediate tuffaceous volcanic rocks with lesser felsic volcanic rocks, although the Kitsault unit is less distinct in field observations from Betty Creek and much more limited in extent and thickness than most described exposures of the Horn Mountain Formation, which can extend for more than 100 km along strike, and are between 1-5 km thick (van Straaten and Nelson, 2016, van Straaten et al., 2022, van Straaten, 2024).

5.4. Lower to upper Hazelton Group transition

Our mapping and geochronological studies suggest that throughout much of the map area there is as much as a 15-20 m.y. gap (Fig. 4) between the top of the Betty Creek Formation of the lower Hazelton Group (ca. 190-192 Ma) and base of the overlying Smithers Formation of the upper Hazelton Group (Toarcian to Bajocian fossils and ca. ≤168.9 Ma detrital zircon). In the Dolly Varden area, the gap may be significantly shorter, with a ≥2.5 m.y. gap between the top of the Betty Creek Formation (ca. 190.5 Ma) and the base of the overlying Spatsizi (ca. ≤188 Ma; Hunter et al., 2022a) and Kitsault units of the upper Hazelton Group. The new ages confirm that the Kitsault unit is only on the western limb and hinge zone of the Mount McGuire anticline and absent at Homestake and at Surebet, where the andesitic volcanic rocks are constrained by the cross-cutting relationship with the Bulldog pluton (Fig. 3; ca. 193.8 Ma). In the Ajax area, along the eastern margin of the map, a fault juxtaposes ca. 198 Ma Betty Creek Formation volcanic rocks against upper Hazelton sedimentary rocks (Upper Jurassic) and obscures the stratigraphic relationships between the upper and lower parts of the Hazelton Group. That the Spatsizi and Kitsault units are limited in extent to the area in the branching termination of the Kitsault River fault suggests deposition and/or preservation related to the faults. In either case, the Kitsault unit represents a volcanic belt prospective for VMS and epithermal mineralization of comparable or slightly older age to VMS mineralization in the Eskay rift (ca. 174-176 Ma; Childe, 1996; Evenchick et al., 2004; Alldrick et al., 2005; Barresi et al., 2015). Further stratigraphic and geochronological studies focused on distinguishing previously unrecognized volcanic rocks of the upper part of the Hazelton Group will be important in assessing the extent of upper Hazelton Group volcanic rocks and their prospectivity for VMS and epithermal mineralization elsewhere in the region.

5.4.1. Smithers Formation and unnamed tuffaceous sedimentary units (Middle-Upper Jurassic)

The laterally extensive fossiliferous sandstone unit of the Smithers Formation (ca. ≤169 Ma; Hunter and van Straaten, 2020) that is characterized by belemnite fossils is conformably overlain by a 250 m to 1,500 m thick unnamed volcano-sedimentary unit with ca. 159 to ≤155 Ma ages. The unit was previously described by Evenchick et al. (2008b) as the Surprise Creek facies of the Salmon River Formation, a formation name that was abandoned by Gagnon et al. (2012). The top of Smithers Formation was considered Middle Jurassic by Gagnon et al. (2012); the Upper Jurassic age reported herein suggests that volcanism started later in the Kitsault River area than in north-central Stikinia. Despite sharing similarities with the Quock Formation (Lower to Middle Jurassic), the unnamed volcanosedimentary unit (Middle to Upper Jurassic) is younger. The felsic tuff and lapilli-tuff layers within the unnamed unit record Late Jurassic magmatism of unknown origin but significantly younger (at least 10 Ma) than volcanism represented by the Kitsault unit. The age recorded by the tuff beds roughly corresponds to Jurassic magmatic pulses in both the eastern (ca. 157-142 Ma) and western (ca. 160-140 Ma) belts of the Coast Plutonic complex (Gehrels et al., 2009).

5.5. Alice Arm and Hyder plutonic suites magmatism and mineralization (Eocene)

Stocks of the Alice Arm plutonic suite host porphyry Mo systems (e.g., Tidewater, Ajax, Bell Moly, Moly May, and Kitsault; Carter, 1981; Orovan et al., 2024). A new age of ca. 55.5 Ma confirms that the rocks hosting the Ajax Mo porphyry are Eocene. The mineralogy of the Ajax stock, in particular the presence of muscovite as an accessory mineral, is similar to that of the peraluminous Moly May pluton 13 km to the southwest of the map area (Abdel-Rahman, 2001). The Moly May pluton has a crustal melting signature that is very distinct from other intrusive bodies in the map area, including the coeval Hyder plutonic suite (Abdel-Rahman, 2001). Future work will seek to determine if the Ajax stock has a similar crustal affinity. The Hyder pluton (ca. 51.9 Ma) and related dikes and sills of the Hyder plutonic suite (ca. 61 to 52 Ma; Evenchick et al., 2008b), cut all other rocks in the map area, and are not known to host significant mineralization.

Mineralization at the Surebet/Golddigger Au-Ag project is Eocene (ca. 51 Ma; Re-Os pyrrhotite; S. Israel, personal comm., January 2024). Located on the margin on the Hyder pluton, it is structurally controlled and hosted in and near faults that cut hornfelsed volcano-sedimentary rocks (S. Israel, personal comm., October 2023) now considered to be in the upper part of the Hazelton Group and, to a lesser extent, volcanic rocks of the Betty Creek Formation (Fig. 3). Mineralization and alteration at Surebet are described as sharing a mutually cross-cutting relationship with dikes and sills that are attributed to the Hyder plutonic suite (Reilly and Lazzarotto, 2023) and are therefore interpreted to overlap in age. The mineralization and alteration is cut by several molybdenum-bearing felsite dikes (Reilly and Lazzarotto, 2023; S. Attersley, personal comm, August 2024) whose descriptions suggest a similar character to the Alice Arm plutonic suite. If these felsite dikes share affinity with the Alice Arm plutonic suite, it may be that the mineralization is coeval with and was possibly generated during the same mineralization event as the Eocene Mo porphyry systems. Regardless, it represents a newly recognized Eocene Au-Ag mineralization style in Upper Jurassic sedimentary strata. It may be that sedimentary rocks in the upper part of the Hazelton Group may have hitherto unrecognized prospectivity for Au-Ag where long-lived faults cut Middle to Upper Jurassic rocks close to prospective Eocene intrusives.

6. Conclusions

The updated geological map and stratigraphic scheme for the Kitsault River area, informed by new U-Pb zircon geochronology, provides a framework for understanding the geological setting of the Hazelton Group, distribution of associated mineral deposits in the Kitsault River area, and provide insights into the regional tectonic history.

The base of the Hazelton Group records the formation of syn-sedimentary fault basins that controlled local deposition of the Kinskuch unit (latest Triassic), which is conformably overlain by the Betty Creek Formation. The Betty Creek Formation records a subsequent period of prolific volcanism (latest Triassic to Early Jurassic) that almost entirely overlaps with ages returned from the coeval Texas Creek plutonic suite (latest Triassic to Early Jurassic). The lower Hazelton Group and Texas Creek plutonic suite are coeval with and host porphyry Au-Cu and epithermal Au-Ag-Cu mineralization in the region (i.e., Big Bulk, Homestake, SanDiego/Red Bluff, Midnight Blue).

The contact between the lower and upper parts of Hazelton Group is interpreted to be unconformable. In the Homestake and Surebet area, there is a time gap of as much as 15-20 m.y. where the Smithers Formation (upper Hazelton Group) directly overlies Betty Creek Formation (lower Hazelton Group). In the Dolly Varden area, where the Spatsizi Formation and Kitsault unit occupy the base of the upper Hazelton Group, the gap may be as short as 1.5 m.y. The Kitsault unit is coeval with VMS and epithermal deposits in the map area (i.e., Dolly Varden, Torbrit, North Star, Wolf, Sault). The spatial association of the Kitsault unit and the VMS deposits with the branching termination of the Kitsault River fault suggests deposition and/or preservation related to long-lived faults.

The Surebet/Golddigger mineralization is coeval with the Alice Arm and Hyder plutonic suites (Eocene) and shares characteristics with late-mineral polymetallic veins described at several Eocene molybdenum porphyry systems in the region. Sedimentary rocks of the upper Hazelton Group may have hitherto unrecognized prospectivity for Au-Ag where faults cut Middle to Upper Jurassic rocks close to prospective Eocene intrusives.

Acknowledgments

We thank the Dolly Varden Silver corporation’s exploration team, in particular Chris Sebert, Rob van Egmond, and Charlie Fleenor for logistical and helicopter support, hospitality staying in their Alice Arm exploration camp throughout fieldwork, and generosity in sharing property-scale geological maps and data. This project benefited from geological discussions with and excellent advice on traverse planning in the area from Chris Sebert. Site visits and discussions with the Goliath exploration team were very helpful. Fantastic field assistance over these last two years of the project was provided by Leonie Ebert, Gabriella Rubinoff, Alexandra Pipe, Bruce Guo, Curran Wearmouth, and Nate Corcoran. Constructive reviews and comments by JoAnne Nelson improved the paper substantially.

References cited

Abdel-Rahman, A.-F.M., 2001. Peraluminous plutonism: nature and origin of the Moly May leucogranite and its Coast Plutonic complex granitic host-rocks, northwestern British Columbia: The Canadian Mineralogist, 39, 1181-1196.

Alldrick, D.J., 1993. Geology and metallogeny of the Stewart mining camp, northwestern British Columbia. British Columbia Ministry of Energy, Mines and Petroleum Resources, British Columbia Geological Survey Bulletin 85, p. 113.

Alldrick, D.J., Dawson, G.L., Bosher, J.A., and Webster, I.C.L., 1986a. Geology of the Kitsault river area (NTS 103P). British Columbia Ministry of Energy, Mines and Petroleum Resources, British Columbia Geological Survey Open File Map 1986-02, 1:50,000 scale, p. 5.

Alldrick, D.J., Nelson, J.L., and Barresi, T., 2005. Tracking the Geology and Mineral Deposits of the Upper Iskut River Area: Tracking the Eskay Rift through Northern British Columbia (104G/1, 2; 104B/9, 10, 15, 16). In: Geological Fieldwork 2004, British Columbia Ministry of Energy, Mines and Petroleum Resources, British Columbia Geological Survey Paper 2005-01, pp. 1-30.

Barresi, T., Nelson, J.L., Dostal, J., and Friedman, R., 2015. Evolution of the Hazelton arc near Terrace, British Columbia: Stratigraphic, geochronological, and geochemical constraints on a Late Triassic-Early Jurassic arc and Cu-Au porphyry belt. In: Gibson H., (Ed.), Canadian Journal of Earth Sciences, 52, pp. 466-494.

Barrett, T.J., and Sherlock, R.L., 1996. Geology, lithogeochemistry and volcanic setting of the Eskay Creek Au-Ag-Cu-Zn deposit, northwestern British Columbia. Exploration and Mining Geology, 5, 339-368.

Carter, N.C., 1981. Porphyry copper and molybdenum deposits, west-central British Columbia. British Columbia Ministry of Energy, Mines and Petroleum Resources, British Columbia Geological Survey Bulletin 64, 81 p.

Childe, F., 1996. U-Pb geochronology and Nd and Pb isotope characteristics of the Au-Ag-rich Eskay Creek volcanogenic massive sulfide deposit, British Columbia. Economic Geology, 91, 1209-1224.

Cohen, K.M., Finney, S.C., Gibbard, P.L., and Fan, J.-X., 2013. The ICS International Chronostratigraphic Chart. Episodes 36, 199-204, 2023 revision. <https://stratigraphy.org/ICSchart/ChronostratChart2023-04.pdf>

Cordey, F., 2020. Report on radiolarians, fieldwork 2017-2019, submission by Emily Miller UBC, 4 samples. Unpublished report EMI-2020-1, Laboratoire de géologie de Lyon Université Claude Bernard Lyon 1, 4 p.

Cordey, F., 2023. Report on radiolarians, fieldwork 2023, submission by E. Miller and B. van Straaten, 6 samples. Unpublished report EMI-2023-2, Laboratoire de géologie de Lyon Université Claude Bernard Lyon 1, 5 p.

Coutts, D.S., Matthews, W.A., and Hubbard, S.M., 2019. Assessment of widely used methods to derive depositional ages from detrital zircon populations. Geoscience Frontiers, 10, 1421-1435.

Cutts, J.A., McNicoll, V.J., Zagorevski, A., Anderson, R.G., and Martin, K., 2015. U-Pb geochronology of the Hazelton Group in the McTagg anticlinorium, Iskut River area, northwestern British Columbia. In: Geological Fieldwork 2014, British Columbia Ministry of Energy and Mines, British Columbia Geological Survey Paper 2015-1, pp. 87-101.

Dawson, G.L., and Alldrick, D.J., 1986. Geology and mineral deposits of the Kitsault Valley. In: Geological Fieldwork 1985, British Columbia Ministry of Energy, Mines and Petroleum Resources, British Columbia Geological Survey Paper 1986-01, pp. 219-224.

Devlin, B.D., and Godwin, C.I., 1986. Geology of the Dolly Varden camp, Alice Arm area. In: Geological Fieldwork 1985, British Columbia Ministry of Energy, Mines and Petroleum Resources, British Columbia Geological Survey Paper 1986-01, pp. 327-330.

Dickinson, W.R., and Gehrels, G.E., 2009. Use of U-Pb ages of detrital zircons to infer maximum depositional ages of strata: A test against a Colorado Plateau Mesozoic database. Earth and Planetary Science Letters, 288, 115-125.

Evenchick, C.A., 1991. Geometry, evolution, and tectonic framework of the Skeena Fold Belt, north-central British Columbia. Tectonics, 10, 527-546.

Evenchick, C.A., 2001. Northeast-trending folds in the western Skeena Fold Belt, northern Canadian Cordillera: A record of Early Cretaceous sinistral plate convergence. Journal of Structural Geology, 23, 1123-1140.

Evenchick, C.A., and McNicoll, V.J., 2002. Stratigraphy, structure, and geochronology of the Anyox Pendant, northwest British Columbia, and implications for mineral exploration. Canadian Journal of Earth Sciences, 39, 1313-1332.

Evenchick, C.A., and Thorkelson, D.J., 2005. Geology of the Spatsizi River map area, north-central British Columbia. Natural Resources Canada, Geological Survey of Canada Bulletin 577, 289 p.

Evenchick, C.A., Mustard, P.S., Porter, S., and Greig, C.J., 1992. Regional Jurassic and Cretaceous facies assemblages, and structural geology in Bowser Lake map area (104A), British Columbia. Natural Resources Canada, Geological Survey of Canada Open File 2582, 17 p.

Evenchick, C.A., McNicoll, V.J., and Snyder, L.D., 2004. Stratigraphy, geochronology, and geochemistry of the Georgie River area, northwest British Columbia, and implications for mineral exploration. Canadian Journal of Earth Sciences, 41, 199-216.

Evenchick, C.A., McMechan, M.E., McNicoll, V.J., and Carr, S.D., 2007. A synthesis of the Jurassic-Cretaceous tectonic evolution of the central and southeastern Canadian Cordillera: Exploring links across the orogen. In: Sears, J.W., Harms, T.A., and Evenchick, C.A., (Eds), Whence the Mountains? Inquiries into the Evolution of Orogenic Systems: A Volume in Honor of Raymond A. Price, Geological Society of America Special Paper 433, pp. 117-145.

Evenchick, C.A., Mustard, P.S., McMechan, M.E., Ferri, F., Ritcey, D.H., Waldron, J.W.F., Porter, S., Greig, C.J., and Smith, G.T., 2008a. Geology, Bowser Lake, British Columbia. Geological Survey of Canada Open File 5706, 1:125,000 scale.

Evenchick, C.A., Mustard, P.S., Greig, C.J., McMechan, M.E., Ritcey, D.H., Smith, G.T., and Ferri, F., 2008b. Geology, Nass River, British Columbia. Geological Survey of Canada Open File 5705, 1:125,000 scale.

Febbo, G.E., Kennedy, L.A., Nelson, J.L., Savell, M.J., Campbell, M.E., Creaser, R.A., Friedman, R.M., van Straaten, B.I., and Stein, H.J., 2019. The evolution and structural modification of the supergiant Mitchell Au-Cu porphyry, northwestern British Columbia. Economic Geology, 114, pp. 303-324.

Gagnon, J.-F., Barresi, T., Waldron, J.W.F., Nelson, J.L., Poulton, T.P., and Cordey, F., 2012. Stratigraphy of the upper Hazelton Group and the Jurassic evolution of the Stikine terrane, British Columbia. Canadian Journal of Earth Sciences, 49, pp. 1027-1052.

Gehrels, G., Rusmore, M., Woodsworth, G., Crawford, M., Andronicos, C., Hollister, L., Patchett, J., Ducea, M., Butler, R., Klepeis, K., Davidson, C., Friedman, R., Haggart, J., Mahoney, B. et al., 2009. U-Th-Pb geochronology of the Coast Mountains batholith in north-coastal British Columbia: Constraints on age and tectonic evolution. Geological Society of America Bulletin 121, pp. 1341-1361.

Giroux, G.H., and L'Heureux, 2007. Update of resource estimation Ajax property Alice Arm, British Columbia, Tenajon Resources Corporation. NI 43-101 Technical Report, 62 p.

Golding, M., 2023. Paleontologogical report on 16 (3 productive) microfossil samples submitted for analysis by B. van Straaten and R. Hunter, British Columbia Geological Survey (2022), Nass River (103P) and Telegraph Creek (104G) map areas. Unpublished report 7-MG-2023, Geological Survey of Canada, 8 p.
Golding, M., 2024. Paleontologogical report on 16 (5 productive) microfossil samples submitted for analysis by B. van Straaten and E. Miller, British Columbia Geological Survey (2023), Nass River (103P) and Telegraph Creek (104G) map areas. Unpublished report 4-MG-2024, Geological Survey of Canada, 9 p.
Golding, M.L., Bringué, M., Cordey, F., and Lei, J.Z.X., 2023. New biostratigraphic data from the northern Canadian Cordillera, British Columbia and Yukon-an update on the Mesozoic Stratigraphy activity of the GEM-GeoNorth Program. Natural Resources Canada, Geological Survey of Canada Open File 9069, 18 p. <publications.gc.ca/pub?id=9.930266&sl=0>
Greig, C.J., and Gehrels, G.E., 1995. U-Pb zircon geochronology of Lower Jurassic and Paleozoic Stikinian strata and Tertiary intrusions, northwestern British Columbia. Canadian Journal of Earth Sciences, 32, 1155-1171.
Greig, C.J., Anderson, R.G., Daubeny, P.H., Bull, K.F., and Hinderman, T.K., 1994. Geology of the Cambria Icefield: Regional setting for Red Mountain gold deposit, northwestern British Columbia. Geological Survey of Canada, Current Research, 1994-A, accessed June 2, 2021, at: <https://doi.org/10.4095/193621>
Greig, C.J., McNicoll, V.J., Anderson, R.G., Daubeny, P.H., Harakal, J.E., and Runkle, D., 1995. New K-Ar and U-Pb dates for the Cambria Icefield area, northwestern British Columbia. Geological Survey of Canada, Current Research, 1995-A, pp. 97-103, accessed June 3, 2021, at: <https://doi.org/10.4095/202764>
Herriott, T.M., Crowley, J.L., Schmitz, M.D., Wartes, M.A., and Gillis, R.J., 2019. Exploring the law of detrital zircon: LA-ICP-MS and CA-TIMS geochronology of Jurassic forearc strata, Cook Inlet, Alaska, USA. Geology, 47, 1044-1048.
Hunter, R.C., and van Straaten, B.I., 2020. Preliminary stratigraphy and geochronology of the Hazelton Group, Kitsault River area, Stikine terrane, northwest British Columbia. In: Geological Fieldwork 2019, British Columbia Ministry of Energy, Mines and Petroleum Resources, British Columbia Geological Survey Paper 2020-01, pp. 101-118.
Hunter, R.C., Sebert, C.F.B., Friedman, R., and Wall, C., 2022a. Geochronologic data from the Kitsault River area, northwest British Columbia. Ministry of Energy, Mines and Low Carbon Innovation, British Columbia Geological Survey GeoFile 2022-13, 4 p.
Hunter, R.C., Sebert, C.F.B., Friedman, R., and Wall, C., 2022b. Revised stratigraphy and geochronology of the Hazelton Group, host rocks for volcanogenic mineralization in the Kitsault River area, northwest British Columbia. In Geological Fieldwork 2021, British Columbia Ministry of Energy, Mines and Low Carbon Innovation, British Columbia Geological Survey Paper 2022-01, pp. 63-81.
LeBel, J.L., 1988. Report on the Tidewater Property Skeena Mining Division British Columbia for Richmark Resources Ltd. British Columbia Ministry of Energy, Mines and Petroleum Resources, Assessment Report 17842, 79 p.
Logan, J.M., and Mihalynuk, M.G., 2014. Tectonic controls on Early Mesozoic paired alkaline porphyry deposit belts (Cu-Au Ag-Pt-Pd-Mo) within the Canadian Cordillera. Economic Geology, 109, 827-858.
Ludwig, K.R., 2003. Isoplot 3.00, A Geochronological Toolkit for Microsoft Excel. University of California at Berkeley. kludwig@bgc.org/isoplot.
Ludwig, K.R., 2012. Isoplot 3.75. A geochronological toolkit for Microsoft Excel. Special Publication, Berkley Geochronology Center, 75 p.
MacDonald, A.J., 1993. Lithostratigraphy and Geochronometry, Brucejack Lake, Northwestern British Columbia. In: Geological Fieldwork 1992, British Columbia Ministry of Energy, Mines and Petroleum Resources, British Columbia Geological Survey Paper 1993-01, pp. 315-324.
Macdonald, A.J., Lewis, P.D., Thompson, J.F.H., Nadaraju, G., Bartsch, R., Bridge, D.J., Rhys, D.A., Roth, T., Kaip, A., Godwin, C.I., and Sinclair, A.J., 1996. Metallogeny of an Early to Middle Jurassic arc, Iskut River area, northwestern British Columbia. Economic Geology, 91, 1098-1114.
MacIntyre, D.G., Ash, C., and Britton, J., 1994. Geological compilation Skeena-Nass area, west central British Columbia. In: British Columbia Ministry of Energy, Mines and Petroleum Resources, British Columbia Geological Survey Open File 1994-14, 1:250,000 scale.
McCuaig, M., and Sebert, C., 2017. 2016 Technical report for the Dolly Varden Property, Skeena Mining Division: British Columbia Ministry of Energy, Mines and Petroleum Resources, Assessment Report 36934, 1123 p.
Miller, E.A., 2023. Emplacement environment and structural modification of the Big Bulk Cu-Au porphyry system, northwestern British Columbia, Unpublished MSc. Thesis, University of British Columbia, 136 p.
Miller, E.A., Kennedy, L.A., and van Straaten, B.I., 2020. Geology of the Kinskuch Lake area and Big Bulk porphyry project: Syndepositional faulting and local basin formation during the Rhaetian (latest Triassic) transition from the Stuhini to the Hazelton Group. In: Geological Fieldwork 2019, British Columbia Ministry of Energy, Mines and Petroleum Resources, British Columbia Geological Survey Paper 2020-02, pp. 77-99.
Miller, E.A., van Straaten, B.I., and Hunter, R.C., 2023. Update on bedrock mapping in the Kitsault River area, northwestern British Columbia. In: Geological Fieldwork 2022, British Columbia Ministry of Energy, Mines and Low Carbon Innovation, British Columbia Geological Survey Paper 2023-01, pp. 23-32.
Miller, E.A., Ferri, M.D., van Straaten, B.I., and Wall, C., 2025. Geochronologic data from the Kitsault River area, northwest British Columbia, Ministry of Mining and Critical Minerals, British Columbia Geological Survey GeoFile, in press.
Nelson, J., and Kyba, J., 2014. Structural and stratigraphic control of porphyry and related mineralization in the Treaty Glacier-KSM-Brucejack-Stewart trend of western Stikinia. In: Geological Fieldwork 2013, British Columbia Ministry of Energy and Mines, British Columbia Geological Survey Paper 2014-1, pp. 111-140.
Nelson, J., Waldron, J., van Straaten, B., Zagorevski, A., and Rees, C., 2018. Revised stratigraphy of the Hazelton Group in the Iskut River region, northwestern British Columbia. In: Geological Fieldwork 2017, British Columbia Ministry of Energy, Mines and Petroleum Resources, British Columbia Geological Survey Paper 2018-1, pp. 15-38.
Nelson, J.L., and van Straaten, B.I., 2020. Recurrent syn- to post-subduction mineralization along deep crustal corridors in the Iskut-Stewart-Kitsault region of western Stikinia, northwestern British Columbia. In: Sharman, E.R., Lang, J.R., and Chapman, J.B., (Eds.), Porphyry Deposits of the Northwestern Cordillera of North America: A 25-Year Update. Canadian Institute of Mining and Metallurgy Special Volume 57, pp. 149-211.
Nelson, J.L., Colpron, M., and Israel, S., 2013. The Cordillera of British Columbia, Yukon, and Alaska: Tectonics and Metallogeny. In: Colpron, M., Bissig, T., Rusk, B.G., and Thompson, J.F.H., (Eds.), Tectonics, Metallogeny and Discovery: The North American Cordillera and Similar Accretionary Settings. Society of Economic Geologists, Special Publication 17, pp. 53-109.
Nelson, J.L., Van Straaten, B., and Friedman, R., 2022. Latest Triassic-Early Jurassic Stikine-Yukon-Tanana terrane collision

and the onset of accretion in the Canadian Cordillera: Insights from Hazelton Group detrital zircon provenance and arc-back-arc configuration. Geosphere, 18, 670-696. Doi: 10.1130/GES02444.1.

Orovan, E.A., Zaborniak, K., and Hooker, K., 2024. Textural evidence for ore fluid transport and the magmatic to hydrothermal transition at the past-producing Kitsault Mo-Ag mine. In: Geological Fieldwork 2023, British Columbia Ministry of Energy, Mines and Low Carbon Innovation, British Columbia Geological Survey Paper 2024-01, pp. 53-64.

Perry, D., and Febbo, G., 2017. Geochemical, Geological, and Geophysical Assessment Report on the Kinskuch Property. British Columbia Ministry of Energy, Mines and Petroleum Resources, Assessment Report 37015, 179 p.

Reilly, J., and Lazzarotto, M., 2023. 2022 Geological, Geochemical, and Diamond Drilling Report on the Golddigger Property, Skeena Mining Division, British Columbia. British Columbia Ministry of Energy, Mines and Petroleum Resources, Assessment Report 41315, 2401 p.

Roth, T., Thompson, J.F.H., and Barrett, T.J., 1997. The precious metal-rich Eskay Creek deposit, northwestern British Columbia. In: Barrie, C.T., and Hannington, M.D., (Eds.), Volcanic Associated Massive Sulfide Deposits: Processes and Examples in Modern and Ancient Settings, Reviews in Economic Geology 8, Society of Economic Geologists, Doi:10.5382/Rev.08.15.

Sebert, C., and Ramsay, A., 2012. Technical Report on the Wolf Deposit 2011 Exploration Program: Geology and Diamond Drilling. British Columbia Ministry of Energy, Mines and Petroleum Resources, Assessment Report 33326, 67 p.

van Straaten, B.I., 2024. Upper Hazelton Group stratigraphy along the Stikine arch, northwestern British Columbia. In: Geological Fieldwork 2023, British Columbia Ministry of Energy, Mines and Low Carbon Innovation, British Columbia Geological Survey Paper 2024-01, pp. 149-177.

van Straaten, B.I., and Nelson, J., 2016. Syncollisional late Early to early Late Jurassic volcanism, plutonism, and porphyry-style alteration on the northeastern margin of Stikinia. In: Geological Fieldwork 2015, British Columbia Ministry of Energy and Mines, British Columbia Geological Survey Paper 2016-1, pp. 113-143.

Swanton, D., Darcy, B., Chris, H., Henry, M., and Jules, L., 2013. 2013 Diamond drilling, geological, geochemical and geophysical report Homestake Ridge project, Located in the Upper Kitsault River Area, Skeena Mining Division, British Columbia. British Columbia Ministry of Energy, Mines and Natural Gas, Assessment Report 34433, 937 p.

Vermeesch, P., 2018. IsoplotR: A free and open toolbox for geochronology. Geoscience Frontiers, 9, 1479-1493.

Vermeesch, P., 2021. Maximum depositional age estimation revisited. Geoscience Frontiers, 12, 843-850.